JOC The Journal of Organic Chemistry

Article

Synthetic Lipomannan Glycan Microarray Reveals the Importance of #(1,2) Mannose Branching in DC-SIGN Binding

Nithinan Sawettanai, Harin Leelayuwapan, Nitsara Karoonuthaisiri, Somsak Ruchirawat, and Siwarutt Boonyarattanakalin

J. Org. Chem., **Just Accepted Manuscript** • DOI: 10.1021/acs.joc.8b02944 • Publication Date (Web): 17 May 2019

ACS Publications

is published by the American Chemical Society. 1155 Sixteenth Street N.W., Washington, DC 20036

Synthetic Lipomannan Glycan Microarray Reveals the Importance of α(1,2) Mannose Branching in DC-SIGN Binding

Nithinan Sawettanai[†], Harin Leelayuwapan[†], Nitsara Karoonuthaisiri[‡], Somsak Ruchirawat[†‖], and Siwarutt Boonyarattanakalin*[§]

[†]Program in Chemical Biology, Chulabhorn Graduate Institute, Chulabhorn Royal Academy, Bangkok 10210, Thailand

[‡]Microarray Laboratory, National Center for Genetic Engineering and Biotechnology (BIOTEC), National Science and Technology Development Agency (NSTDA), Pathum Thani 12120, Thailand

[‖] Laboratory of Medicinal Chemistry, Chulabhorn Research Institute, and Centre of Excellence on Environmental Health and Toxicology Bangkok 10210, Thailand

[§]School of Bio-Chemical Engineering and Technology, Sirindhorn International Institute of Technology, Thammasat University, Pathum Thani 12121, Thailand

*Corresponding Author, E-mail: siwarutt@siit.tu.ac.th, siwarutt.siit@gmail.com

ABSTRACT

Lipomannan (LM), a glycophospholipid found on the cell surface of mycobacteria, involves the virulence and survival in host cells. However, there is little to no information on how exactly mannan alignment, including the number of mannose units and the branched motif of LM, affects protein engagement during host pathogen interactions. In this study, we synthesized the exact substructures of the LM glycan which consist of an α(1,6) mannan core, with and without the complete α(1,2) mannose branching, and comparatively studied their protein-carbohydrate interactions. The synthetic LM glycans were equipped with a thiol linker for immobilizations on the surfaces of microarrays. As per our findings, the presence of the branching α(1,2) mannose on the LM glycans increases their binding toward DC-SIGN receptor. An increase in the number of mannose units on the glycans also increases the binding with the mannose receptor. Thus, the set of synthetic glycans can serve as a useful tool to study the biological activities of LM and can provide better understanding of host-pathogen interactions.

INTRODUCTION

Tuberculosis (TB) is a severe airborne infectious disease that is caused by a single infectious agent—*Mycobacterium tuberculosis* (Mtb). In 2017 alone, approximately 10.0 million people developed TB.[1] There were 1.3 million deaths from TB among HIV-negative people and an additional 300,000 deaths among HIV-positive people.[1] Mtb has unique cell wall characteristics, including a thick layer of lipid conjugated with a complex array of glycans. During an infection, lipomannan (LM) is one of the key cell surface glycophospholipids implicated in the virulence and survival of the mycobacteria in the host's mammalian cells.[2,3]

The structural features of LM from the Mtb surface are illustrated in Figure 1. The LM structure consists of a phospholipid, a lipidated mannose, and a complex polymannan attached to the *myo*-inositol at 1-*O*, 2-*O*, and 6-*O* positions, respectively. The polymannan residue is composed of an α(1,6) linked backbone branched with additional mannose units at the 2-*O* position.[4,5] The numbers and positions of the acyl chains vary for different strains of mycobacteria. The acyl chains can be attached to the glycerol unit and the mannose on the 2-*O* position of the inositol.[6]

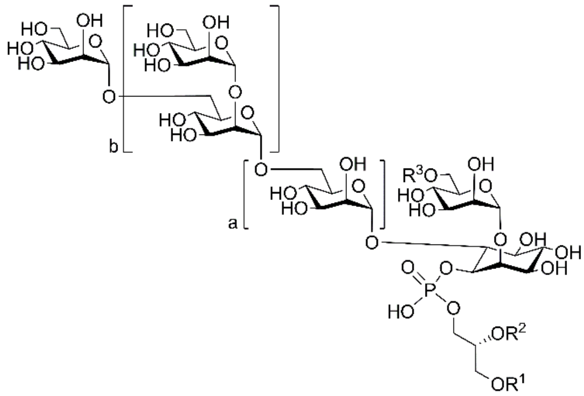

Figure 1. Structural features of the lipomannan (LM) of *Mycobacterium tuberculosis* (Mtb).[7] Glycan is composed of an α(1,6) mannosyl backbone branched with additional mannose units at the 2-*O* position (a and b are varied; R^1 is tuberculostearic acid, R^2 and R^3 are various fatty acids).

LM is a highly active pro-inflammatory activator when compared to other mycobacteria surface glycolipids. Lipoarabinomannan (LAM) was unable to stimulate a significant cytokine secretion. The cytokine expression increased after the chemical degradation of the arabinan chain of LAM to reveal the core LM[8] and the mutation of mycobacterial LAM with a truncated arabinan domain.[9] The results indicate that the arabinan portion of LAM may cover the LM structure and thus blocks the immunostimulatory effects.

Despite LM being isolated from different species of mycobacteria, LM were potent inducer of interleukin-12 (IL-12) and apoptosis[10], and it causes the secretion of interleukin-8 (IL-8) and tumor necrosis factor alpha (TNF-α).[8] The precursor of LM, phosphatidyl-*myo*-inositol dimannoside (PIM_2), has been proven to show no activity.[8,10] Thus, it can be inferred that the activity of LM must arise from the mannan core of LM which consists of the α(1,6) mannan backbone and multiple monosaccharide branching.

The role of α(1,2) mannose branching was studied in the *Mycobacterium marinum* zebrafish infection model. A disruption of *M. marinum mptC* (α(1,2) mannosyltransferase) caused the mutant to lack the mannose caps on LAM and α(1,2) mannose branching on the mannan core of LM. The *M. marinum mptC* mutant was strongly attenuated in the zebrafish. To clearly observe the effect of mannose core branching, the *M. smegmatis mptC* gene was introduced into the mutant to restore the branching. Restoring the mannan core branching but not the mannose cap elongation could fully complement the virulence defect in embryonic zebrafish. These results show that α(1,2) mannose branching, and not the mannose cap, play an important role in mycobacterial pathogenesis in the context of innate immunity.[11]

An alteration of the lipomannan structure by hypermannosylation could enhance innate immune responses. The deletion of the glycosyltransferase, *NCgl2096*, from *Corynebacterium glutamicum* that encodes for an α(1,2) arabinofuranosyltransferase, resulted in the absence of arabinose from LAM and the additional mannosylation of the branching sites. Such hypermannosylated LM was a stronger inducer of cytokine responses than LAM in both *in vitro* and *in vivo*.[12]

With its strong pro-inflammatory activity and uniqueness of structure that is found to be common in every species of mycobacteria, LM becomes an interesting molecule to study as a potential antigen and/or adjuvant for vaccine development. However, the extraction of LM from a mycobacterial cell wall is a tedious process and even the most efficient methods usually only yield small amounts of the product with contaminations.[13] Moreover, the uncertainty of the exact structure limits the use of isolated LM in structure-activity relationship (SAR) studies and immunological studies. SAR studies that employ computational chemistry can only be done precisely if they use a well-characterized target structure.[14] The chemical synthesis approach offers a defined structure of LM with high purity and yield. An efficient chemical synthesis of LM compound from *n*-pentenyl orthoesters facilitated by the use of ytterbium triflate/*N*-iodosuccinimide has been reported.[15] The exact structure of the synthetic LM can be used as a biochemical tool to study the interactions between the Mtb surface components and the human immune system. A better understanding of such interactions is essential for the development of preventive measures and treatments for TB.

The chemically defined exact structures of the LM glycan, which is an α(1,6) mannan core with and without the complete α(1,2) mannose branching, have never been synthesized and comparatively investigated for its immunological properties before this study. To observe the effect of LM α(1,2) mannose branching and the size of the α(1,6) mannoside core, we performed systematic investigations on the syntheses and immune receptor bindings of the different patterns of the LM glycans. The comparisons were done among the linear α(1,6) mannosides at different chain lengths and the corresponding α(1,2) mannose branching on the linear mannoside core (Figure 2). There are four different patterns of synthetic glycans. The linear α(1,6) mannosides, consisting of 2 and 5 units, are a feature of the targets—**Man$_2$** and **Man$_5$**. The complete mannosylation at the 2-*O*-positions of the linear di- and pentamannosides backbone gives rise to the branched targets—**BMan$_4$** and **BMan$_{10}$**, respectively.

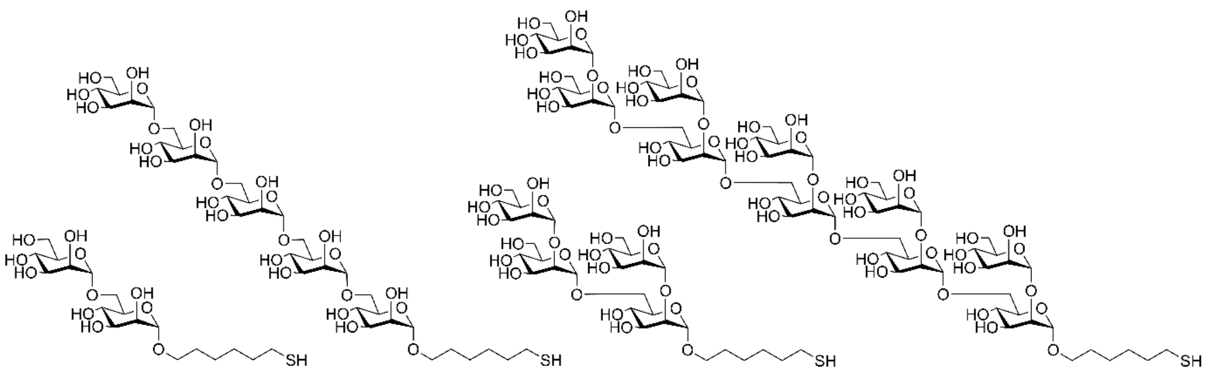

Man$_2$ Man$_5$ BMan$_4$ BMan$_{10}$

Figure 2. Structures of synthetic LM glycans, with and without branched mannose at C-2.

The synthetic glycans were equipped with a thiol linker to facilitate the process of glycan immobilization on the solid surfaces and on the proteins. The bindings of the different synthetic glycans with dendritic cell-specific intercellular adhesion molecule-3 grabbing nonintegrin (DC-SIGN) and mannose receptors, which are the key immune receptors on dendritic cells, were studied side by side by microarrays. The experimental results would determine whether, and to what extent, the α(1,2) mannose branching pattern is implicated during immune receptor binding. The synthetic glycans are useful for various biological and immunological studies of lipomannan. This study provides a better understanding of the interactions between the pathogen and the host's immune system.

RESULTS AND DISCUSSION

Retrosynthetic Analysis

The overall structure of the synthetic targets was obtained by the convergent assembly of the mannosyl residue and a thiol linker (Scheme 1). The key steps in these syntheses are the glycosylation of the mannosyl acceptors and donors to construct the linear and branched mannoside patterns. The linear pentamannoside is derived from the coupling of trimannoside **3** and dimannosyl imidate **4**, which can be prepared from three mannosyl building blocks (compounds **1, 5,** and **6**). The coupling of the linear mannosyl residue with the thiol linker **2** by a glycosidic bond affords the masked linear di- and pentamannosides—**Man$_2$** and **Man$_5$**, respectively. Further complete glycosylation at the 2-*O*-position of the linear backbone mannose with mannosyl phosphate **1** gives rise to the masked branched di- and branched pentamannosides—**BMan$_4$** and **BMan$_{10}$**, respectively. The protecting groups were globally removed by Birch reduction to yield the unmasked target compounds. The synthetic approach in this project is highly convergent, relying on only four types of building blocks, all of which can be synthesized in parallel without relying on one another.

Scheme 1. Retrosynthetic analysis for the assembly of synthetic targets

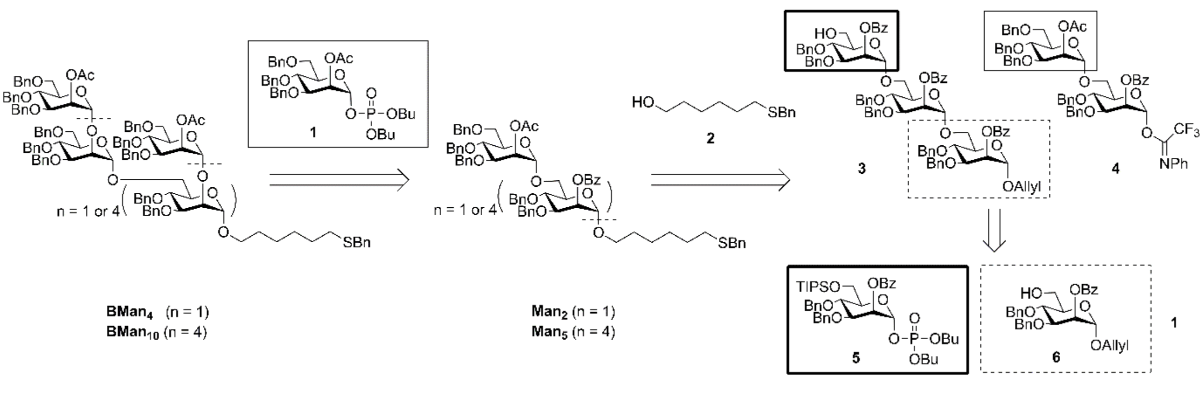

The glycosylation of the linear mannosyl residue and the thiol linker needed to be done prior to the installation of the branching α(1,2) mannose in order to form an alpha glycosidic bond. The stereoselectivity of every glycosidic bond formation is ensured by neighboring C-2 ester protecting groups which are either *O*-benzoyl or *O*-acetyl groups. Consequently, the nucleophile (thiol linker or mannosyl acceptor) necessarily approach the activated mannoside from the bottom face because the top face is not accessible. This leads to alpha glycosidic bond formations.

Assembly of Oligomannoside Fragments

Only three types of mannosyl building blocks were needed to prepare mannosides in the series in this study. The preparation of trimannoside **3** required two cycles of glycosylation in the presence of TMSOTf (Scheme 2). To allow the formation of two glycosidic bonds in the α(1,6) direction, mannosyl phosphate **5** was used to synthesize trimannoside **3**. Mannosyl building blocks **5** and **6** were first assembled to give disaccharide **7** at 75% yield. Due to TMSOTf, the TIPS group was also removed. The glycosylation of dimannoside **7** with mannosyl phosphate **5** provided trimannoside **3** at 66% yield. A formation of oligomers might occur but did not appear as a major side product. It is possible that the TIPS removal occurred after the glycosylation had almost completed. The glycosylation reaction was also controlled to limit the formation of oligomers by conducting the reaction at low temperature, maintaining the temperature uniformly throughout the reaction time, and holding the reaction time for not too long.

Not all of mannose **6** was coupled with mannosyl phosphate **5** during the first glycosylation. The remaining mannose **6** had to be completely removed before another glycosylation; otherwise it would form dimannoside **7** which was co-eluted with trimannoside **3** during the purifications by silica gel column chromatography and size exclusion chromatography. Using the newly prepared mannosyl phosphate **5** also facilitated glycosylation by increasing the reaction yield.

Scheme 2. Synthesis of trimannoside **3**[a]

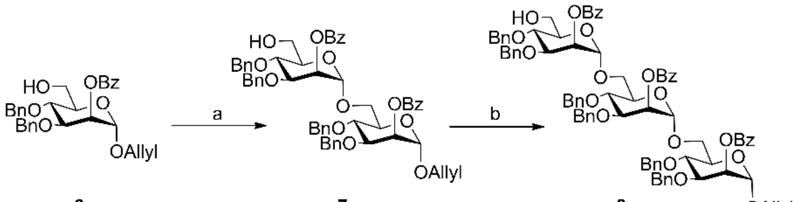

[a] Reagents and conditions: (a) **5** (1.3 equiv.), TMSOTf, CH_2Cl_2, 0 °C, 75%; (b) **5** (1.2 equiv.), TMSOTf, CH_2Cl_2, 0 °C, 66%.

Dimannoside **8** was obtained by glycosylation between mannosyl building blocks **1** and **6** by TMSOTf activation (Scheme 3). Mannosyl phosphate **1** was suitable to be the terminal unit of the non-reducing end of mannose because **1** has a permanent protecting group (*O*-benzyl group) at the C-6 position and a temporally *O*-acetyl group at the C-2 position for further branching mannosylation. Removal of the allyl group of compound **8** was efficiently conducted using palladium chloride. The *N*-phenyltrifluoroacetimidoyl group was then installed at the C-1 position of compound **9** to provide the leaving group for dimannoside **4**. The union of dimannosyl imidate **4** and trimannoside **3**, using standard TMSOTf-catalyzed glycosylation, furnished pentamannoside **10** (Scheme 3). The allyl group of compound **10** was cleaved and replaced with the *N*-phenyltrifluoroacetimidoyl group to provide the site for the attachment with the thiol linker moiety.

Scheme 3. Assembly of oligosaccharide donors **4** and **12**[a]

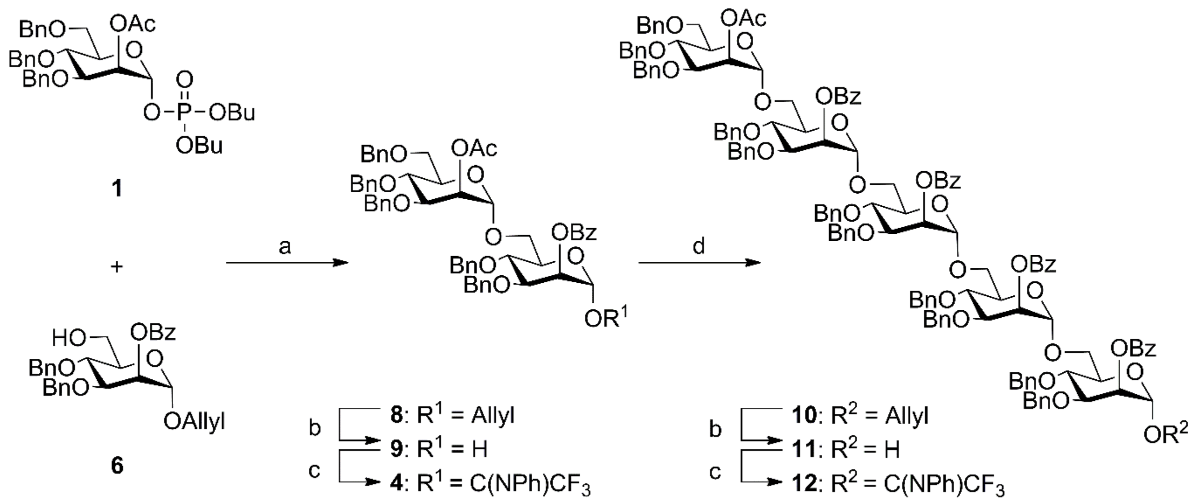

[a] Reagents and conditions: (a) TMSOTf, CH_2Cl_2, 0 °C (Molar ratio **1**:**6** = 3:2), 99%; (b) $PdCl_2$, NaOAc, AcOH, rt, 87% for **9** and 85% for **11**; (c) $CF_3(Cl)CNPh$, Cs_2CO_3, Acetone, 0 °C, 85% for **4** and 65% for **12**; (d) **3**, TMSOTf, CH_2Cl_2, 0 °C (Molar ratio **4**:**3** = 3:2), 88%.

The removal of the allyl protecting group on the reducing end of compound **8** with catalytic $Pd(OAc)_2$, PPh_3, and Et_2NH yielded 60% of hemiacetal **9** (Scheme 3). $Pd(OAc)_2$ (2 equiv.) in MeOH (1 mL) was allowed to form a complex with PPh_3 (6 equiv.) for 6 hours prior to the addition of Et_2NH (6 equiv.) and the starting material (~100 mg) at room temperature (rt). The reaction solution was further stirred for 12 hours to convert compound **8** to compound **9**. Palladium residues remained with the compound even after filtration through a pad of Celite and purification by a silica gel column chromatography. Using $PdCl_2$ under the buffered conditions of AcOH and NaOAc (pH 2 after mixing) was a better way to remove the allyl group. Palladium residue was more easily removed by filtration through a pad of Celite. The reaction could be finished in one step (12 h), and the reaction yield increased to 87% for compound **9** (Scheme 3). A small amount of the side product from the Wacker-type oxidative side reaction also formed during the Pd-mediated anomeric deallylation. The corresponding ketone product could be observed by mass spectrometry and as a minor spot on Thin Layer Chromatography (TLC).

The syntheses of mannosyl imidates **4** and **12** were achieved by the treatment of hemiacetals **9** and **11** with *N*-phenyltrifluoroacetimidoyl chloride under basic conditions (Scheme 3). Cs_2CO_3 proved to work better than K_2CO_3 and provided compounds **4** and **12** at 72% and 51%, respectively. Due to the acidic conditions of the deallylation step, the crudes of hemiacetals **9** and **11** were neutralized prior to the installation of the imidates. Adjusting the reaction pH to 7 by Na_2CO_3 improved the yields to 85% and 65%, respectively.

Assembly of Mannosides with a Thiol Linker and Branching

The thiol terminated linker **2** was prepared from 6-mercapto-1-hexanol by benzylating the thiol functional group with benzyl bromide.[16] The assembly of mannosyl residue and the thiol linker was done by glycosylation (Scheme 4). *N*-phenyltrifluoroacetimidoyl mannosides (compounds **4** and **12**) were treated with thiol linker **2** in the presence of TMSOTf to afford compounds **13** and **16** in good yield. Mannosyl imidates **4** and **12** were treated with an excess amount of the thiol linker (5 equiv.) to increase the linker glycosylated product yields. However, there was some difficulty in separating the excess linker from mannosides **13** and **16**. The thiol linker was co-eluted with products during silica gel column chromatography despite the moderate difference in R_f values. The excess thiol linker is needed to be separated from oligomannosides using size exclusion column chromatography. Silica gel column chromatography was then used to separate the products **13** and **16** from the corresponding hemiacetal byproducts.

Removing all of the protecting groups by Birch reduction gave rise to the final products: linear di- and pentamannosides, equipped with a thiol linker (**Man$_2$** and **Man$_5$**, Figure 2). In parallel, hydrolyzing the *O*-acetyl and *O*-benzoyl groups of compounds **13** and **16** by refluxing with NaOMe at 50 °C gave mannan intermediates **14** and **17**. The free C-2 hydroxyl groups on mannan intermediates **14** and **17** were able to accept mannoside **1** to form the branched targets (Scheme 4). The α(1,2) branched mannosylation by mannosyl phosphate **1** with TESOTf as a catalyst yielded compounds **15** and **18**. The global protecting group removals provided the final products, which are branched di- and branched pentamannosides, equipped with a thiol linker (**BMan$_4$** and **BMan$_{10}$**, Figure 2).

Scheme 4. Conjugation of mannosides with a thiol linker and the removal of protecting groups using Birch reduction[a]

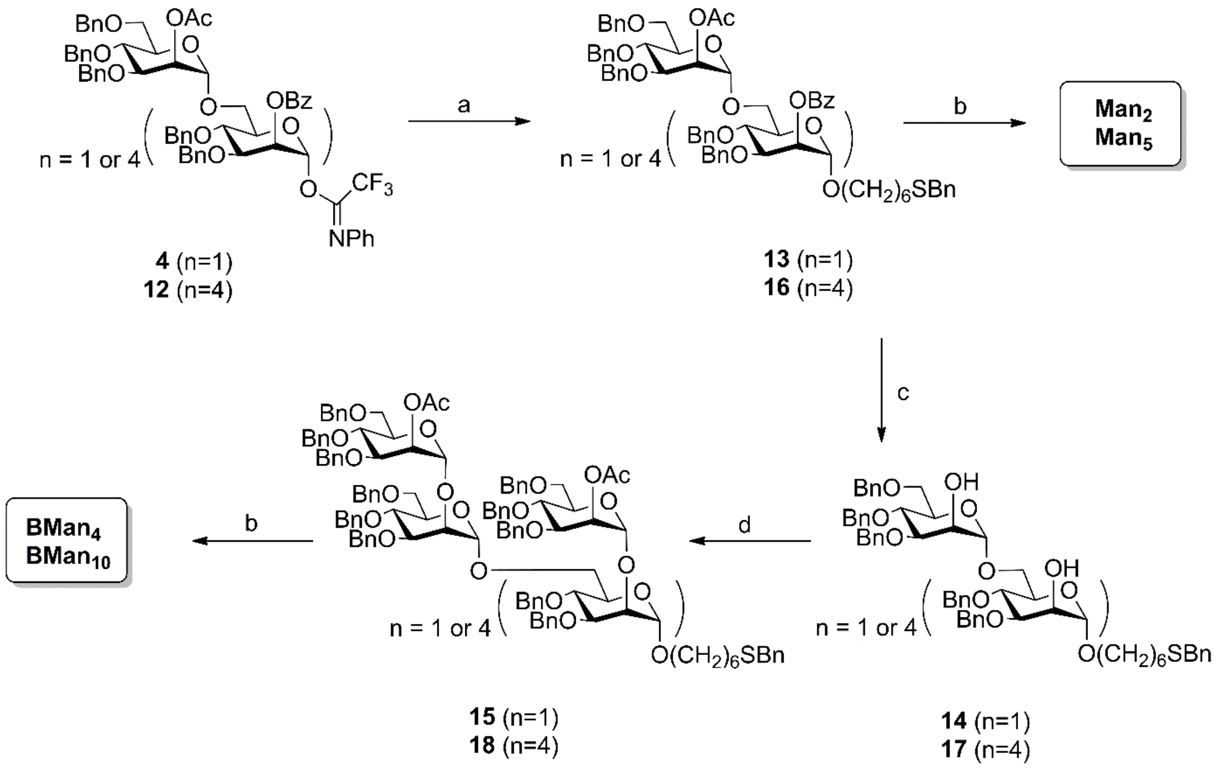

[a] Reagents and conditions: (a) **2** (5 equiv. for **4** and 4 equiv. for **12**), TMSOTf, CH_2Cl_2, -10 °C, 77% for **13** and 76% for **16**; (b) Na, NH_3 (l), THF, -78 °C, 25% for **Man$_2$**, 27% for **Man$_5$**, 33% for **BMan$_4$** and 31% for **BMan$_{10}$**; (c) NaOMe, CH_2Cl_2, MeOH, 50 °C, 93% for **14** and 94% for **17**; (d) **1** (5 equiv.), TESOTf, Et_2O, 0 °C, 88% for **15** and 60% for **18**.

Branching α(1,2) mannose was installed completely onto all the C-2 hydroxyl groups on intermediates **14** and **17,** as confirmed by NMR spectroscopy. The ^{1}H NMR of compound **15** displays four anomeric proton signals at 5.08, 5.07, 4.92, and 4.76 ppm; the ^{13}C NMR shows four anomeric carbon signals at 99.59 (two overlapping), 98.51, and 98.42 ppm. Similarly, the ^{1}H NMR of compound **18** shows ten anomeric proton signals between 5.12 and 4.88 ppm. Ten anomeric carbon signals between 99.90 and 98.70 ppm are found in the ^{13}C NMR spectrum. The molecular weights of **15** and **18** were also confirmed by high resolution mass spectrometry ($[M+Na]^+$ calculated for **15**:1969.8621, found 1969.8616; and $[M+2Na]^{2+}$ calculated for **18**: 2220.9524, found 2220.9544).

For the global protecting group removal by Birch reduction, both linear mannan intermediates (**13** and **16**) and branched mannan intermediates (**15** and **18**) were treated with sodium in liquid ammonia to yield the final products at around 30% yields. Some of the starting materials and the partially unmasked products remained in the organic layer after extracting the aqueous layer of the crude product with CH_2Cl_2. The side products were subjected to Birch reduction again to convert them into the desired products. The unmasked final products were achieved as a mixture of a single molecule and the corresponding disulfide dimer. The molecular peak of each product was found by MALDI-TOF mass spectroscopy as reported in the Experimental section. Moreover, the mass peak of each corresponding disulfide dimer was also found as the followings: $[2M+Na]^+$ calculated for dimer for **Man$_2$**: 937.3385, found 937.3356; $[2M+H]^+$ calculated for dimer of **Man$_5$**: 1887.6735, found 1887.6759; $[2M+Na]^+$ calculated for dimer of **BMan$_4$**: 1585.5498, found 1585.5461; and $[2M+2Na]^{2+}$ calculated for dimer of **BMan$_{10}$**: 1776.5867, found 1776.5878.

The final products in this study were synthesized in a stepwise approach which resulted in chemically well-defined structures. According to the ^{1}H NMR spectroscopic data, all of the protecting groups were removed completely as the aromatic and acetate peaks disappeared. The integrated areas of the anomeric protons correspond to the number of mannosyl units in each compound of the final products. The ^{1}H NMR anomeric signals are displayed as two discrete peaks at 4.89 and 4.84 ppm with the integrated area of 2 for **Man$_2$** and are displayed as two overlapping peaks at 4.87 and 4.83 ppm with the integrated area of 5 for **Man$_5$**. For the branched mannoside products, the anomeric peaks shift to lower field. The ^{1}H NMR chemical shift of the anomeric protons are at 5.12, 5.06, and 5.01ppm for **BMan$_4$** and at 5.11, 5.07, 5.03, and 4.90 ppm for **BMan$_{10}$**, of which the areas under peaks correspond to the 4 and 10 mannosyl residues, respectively. High resolution mass spectrometry of the final products confirms their expected exact masses to be the following: $[M+Na]^+$ calculated for **Man$_2$**: 481.1720, found 481.1739; $[M+Na]^+$ calculated for **Man$_5$**: 967.3304, found 967.3343; $[M+Na]^+$ calculated for

BMan$_4$: 805.2776, found 805.2798; and $[M+Na]^+$ calculated for **BMan$_{10}$**: 1777.5945, found 1777.5980. MALDI-TOF mass spectra of the final products were obtained in a positive mode using 2,5-dihydroxybenzoic acid (DHB) as the matrix.

All of the glycosidic bonds were formed in alpha configuration as a result of the neighboring acyl group participation. The stereoselectivity was evidenced by the measurement of the coupling constants between the anomeric carbon and the corresponding anomeric proton ($J_{C1,H1}$). The typical $J_{C1,H1}$ value for alpha mannoside is 171 Hz and for beta mannoside is 159 Hz.[17,18] The $J_{C1,H1}$ in all mannosides, with and without protecting groups, are between 171-173 Hz, which corresponds to the typical values of alpha mannoside.

Mannan Microarrays to Determine Bindings to DC-SIGN and MR

Interactions between the mycobacterium cell membrane and immune receptors determine the immunomodulatory outcomes of Mtb. These protein-carbohydrate interactions play a key role in the infectious, virulent, and survival events of Mtb in mammalian host cells.[19-21] Subtle variations in the LM structure, with regard to the mannan chain lengths, along with the pattern of the glycan alignment present in LM, dramatically impact LM's unique roles in immunoregulation.[8,10,22-24] Several studies have addressed the significance of the mannan motif present in LM toward pro-inflammatory activities;[8,10,22,25] however, insights into how exactly the mannan alignment affects protein engagement have never been revealed. Thus, it was vital to determine how different LM substructures affect biological interactions. To gain a better understanding of the protein-carbohydrate interactions, a carbohydrate microarray was assembled as a biochemical tool to study the influence of the linear α(1,6) mannan, along with branching α(1,2) mannan present in LM, on their binding affinities with the relevant immune receptors, DC-SIGN and MR.

DC-SIGN and MR are important pattern-recognition receptors of antigen presenting cells. DC-SIGN and MR contribute to the initiation of pro-inflammatory responses, and antigen internalization and later presentation to lymphocytes, which trigger an adaptive immune response. DC-SIGN and MR targeting is an efficient strategy of pathogens like Mtb and HIV to evade the immune system.[2,26-28] Mannosylated moieties on the mycobacterial cell wall have previously been shown to exploit these receptors to enter antigen presenting cells.[2,26,28-30] However, the interactions between the chemically defined LM glycan, with and without α(1,2) branched mannose, with DC-SIGN and MR have never been comparatively investigated before.

The synthetic LM glycans were already equipped with a thiol linker for immobilization on the maleimide-functionalized microarray surfaces. The glass slides printed with the synthetic glycans were incubated with the target receptors in a buffer solution at rt to allow the receptors to bind to the immobilized LM glycans. Excess receptors were washed off and the remaining bound receptors were detected through incubation with the fluorescein-conjugated antibody. The α(1,6) mannan chain with 13 repeating units (**Man13**)[18] was also investigated in parallel as a positive control for comparison, in order to assess the effects of the differing numbers of mannose units and the α(1,2) branched mannosyl pattern. The synthetic LM glycans bound to both DC-SIGN and MR in a specific manner (Figure 3), which was statistically significant when compared to the fluorescence levels of the thiol linker and the buffer (negative controls). As expected, the linear α(1,6) mannan chain with 13 repeating units bound significantly to both receptors. The binding affinity of MR increased with the number of mannose units on the glycan. The increase in the observed fluorescence intensities is in line with the increase in the numbers of mannose units of the polysaccharides (**Man13** > **BMan10** > **Man5** > **BMan4** > **Man2**).

Previous studies of lectin binding interactions with Mtb have suggested that α(1,2) terminal mannose residues on LAM are responsible for the engagement.[2,28-30] From our microarray results, MR recognized the mannan well and the binding was enhanced when the units of mannose were increased, but the enhancement was not necessarily specific to α(1,2) or α(1,6) linkage. Multiple C-type carbohydrate recognition domains (CRDs) of MR are required to achieve tight binding to multivalent ligands unit.[31,32] Multiple CRDs are arranged spatially to accommodate the geometric configurations of natural oligosaccharides.[31,32] In this case, the increasing in terminal mannose units in α(1,2) branched structure might not create the conformation that favors MR-carbohydrate interactions. It was also shown by Geijtenbeek *et al.* that ManLAM (with α(1,2) terminal mannose units) bound to dendritic cells preferably through DC-SIGN, not MR.[2] The presence of the α(1,2) mannose branching pattern on the LM glycan significantly increased the binding ability of the LM glycan with DC-SIGN (Figure 3). When comparing mannans with the same backbone lengths (**Man5** Vs. **BMan10** and **Man2** Vs. **BMan4**), the mannans with the α(1,2) mannose branching motif strikingly bound with DC-SIGN with higher affinity (**BMan10** > **Man5** and **BMan4** > **Man2**). This implies that the increase in the observed fluorescence intensities profoundly depends on the increase in the numbers of α(1,2) mannose branching units of the polysaccharides rather than the total number of mannose units of the polysaccharides. For example, **BMan10** binds with DC-SIGN at a higher affinity than **Man_{13}**, although **$BMan_{10}$** contains fewer mannan repeating units than **Man_{13}** does. The same thing is also true for a higher DC-SIGN affinity of **$BMan_4$**, as compared to that of **Man_5**. This suggests that the α(1,2) mannose branching motif and α(1,6) mannan chain could be a key mycobacteria glycan epitope that can be recognized and detected by the human immune receptors DC-SIGN and MR, respectively.

Several publications suggested that high mannose oligosaccharides interact with DC-SIGN in multiple orientations resulting in statistical affinity enhancements.[33-36] The different binding orientations feature contacts between mannan and different regions of the protein at the same time. The multiple interactions occur more likely due to the more available mannose units on larger mannan and/or the branched mannan. The observed microarray fluorescence intensities suggested that other contacts between DC-SIGN's carbohydrate recognition domains and mannan might occur and provide substantial affinity enhancements.

Blattes *et al.* studied different types of mannodendrimers binding affinity toward DC-SIGN.[37] Spatial geometry, and stereo- and regiochemistry of glycan have strong influences on lectin binding. Subsequently, density also play a role in determining the spatial geometry of glycan. The optimal glycan density would create a perfect environment for lectin binding.[32,38,39] The fluorescent intensities that showed dose independent are probably because at the lower printing concentrations, glycan molecules might already saturate the array surface. Thus, glycan-protein interactions reached their saturation point. Consequently, there was no significant difference on the protein binding affinity among different concentrations of the same glycan structure.

The activation of macrophages and dendritic cells depends on the net balance between positive and negative signals. The results from this study underscore the significance of the linear α(1,6) mannan and the α(1,2) branched mannosyl pattern presented in the LM structures and highlight their potential use as an immune modulator that may exert desired immunological properties such as adjuvant activities. Studies of these interactions may lead to the development of novel, effective, and highly selective therapeutic practices.

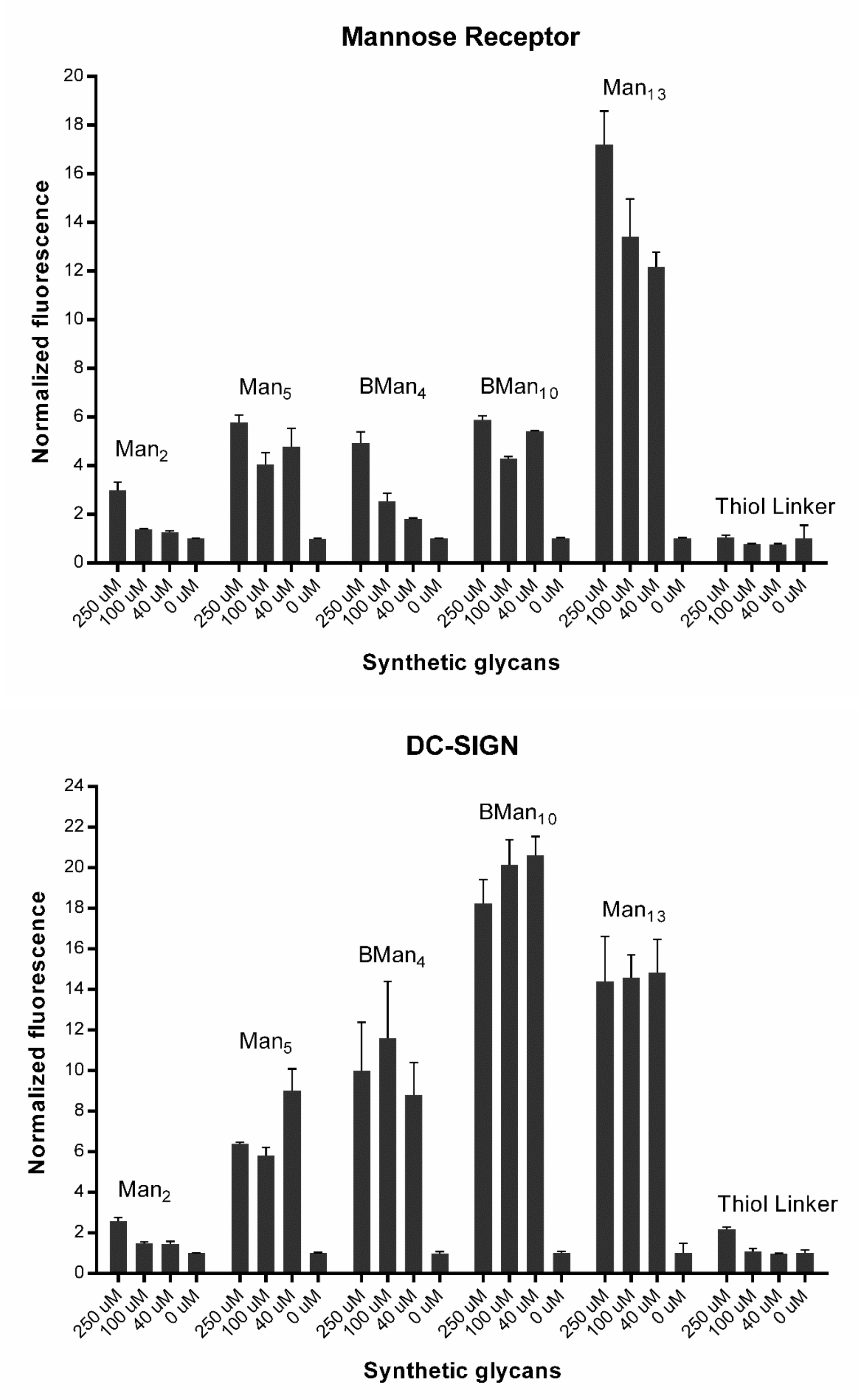

Figure 3. Analysis of MR and DC-SIGN bindings with synthetic Mtb glycan substructures at various printing concentrations. Fluorescence intensity was normalized with buffer spots. Data are presented as mean±SD for each triplicate.

CONCLUSION

In this study, we have developed an efficient synthesis of the α(1,6) mannan cores and the chemically exact α(1,2) mannosyl branch on the α(1,6) mannan cores. The synthetic glycans serve as biochemical tools to determine the effects of mannosyl unit lengths and the branched motif of the Mtb LM on the binding with DC-SIGN and mannose receptors. The stepwise synthetic strategy is highly convergent, relying on only three types of mannosyl acceptors and donors which can be prepared from a mannosyl tricyclic orthoester. Each synthetic LM glycan was equipped with a thiol linker at the reducing end of the mannan to be immobilized on its surface for a carbohydrate microarray. The results show that the presence of the branching α(1,2) mannose motif on the LM glycan, which is more important than the total number of mannose units, enhances the binding affinity toward the relevant immune DC-SIGN receptor. Additionally, the more mannose units on the glycans, though not necessarily specific to α(1,2) or α(1,6) linkage, result in the greater the binding with the mannose receptor. Thus, synthetic LM glycans could serve as a biochemical tool for further studies. This experiment provides a much better understanding of the protein-carbohydrate interactions between the pathogens and the host's immune system.

EXPERIMENTAL SECTION

General information for Chemical Synthesis

All the chemicals used were reagent grade and used as supplied, except where noted. All the reactions were performed in oven-dried glassware under an inert atmosphere, unless noted otherwise. Dry dichloromethane (CH_2Cl_2) was obtained from a solvent purification system (PureSolv MD 5, Innovative Technology). Benzyl bromide was treated with aluminum oxide prior to use. Analytical thin layer chromatography (TLC) was performed on Merck silica gel 60 F_{254} plates (0.25 mm). Compounds were visualized by staining with cerium ammonium molybdate (Hanessian's Stain) solution. Flash column chromatography was carried out using a forced flow of the indicated solvent on Fluka Kieselgel 60 (230-400 mesh). Gel filtration chromatography was carried out using Sephadex LH-20 from Biosciences.

All the new compounds were characterized by NMR spectroscopy (^{1}H, ^{13}C), ESI-MS, MALDI-TOF, optical rotation, and melting point (for a solid). NMR spectra were recorded on Bruker AVANCE III (300 MHz), Bruker Fourier 300 (300 MHz), and Bruker AVANCE 400 (400 MHz) spectrometer. NMR chemical shifts (δ) are reported in ppm relative to internal standards ($CDCl_3$, δ 7.26 ppm for ^1H, and δ 77.00 ppm for ^{13}C; D_2O, δ 4.79 ppm for ^1H) and coupling constants (*J*) are reported in Hz. Splitting patterns are indicated as s, singlet; d, doublet; t, triplet; q, quartet; m, multiplet; brs, broad singlet for ^1H NMR data. High resolution ESI mass spectra were obtained by Bruker microTOF mass spectrometer and Thermo Scientific Q Exactive Focus Orbitrap mass spectrometer. MALDI-TOF was carried out using JEOL JMS-S3000 MALDI-TOF mass spectrometer and Shimadzu AXIMA Performance MALDI TOF-TOF mass spectrometer. Optical rotations were measured using JASCO P-1020 polarimeter. Melting points were measured in capillaries using Staurt SMP30 apparatus.

General Procedures for Glycosylations

The mannosyl donor and acceptor were co-evaporated with anhydrous toluene three times *in vacuo* and placed under high vacuum for at least 4 h. Glycosylations were performed without molecular sieves. Under argon atmosphere, a solvent was added to the mixture of starting materials at rt and the solution was cooled to the desired temperature (0 °C by ice-water bath and -10 °C by ice-acetone bath). A promoter (TMSOTf or TESOTf) was introduced to the reaction solution in one portion via syringe. After the reaction had finished, excess triethylamine (NEt_3) was added to quench the reaction at the particular reaction temperature. The reaction mixture was concentrated *in vacuo* and purified by flash silica gel column chromatography.

Allyl *O*-(2-*O*-Benzoyl-3,4-di-*O*-benzyl-α-D-mannopyranosyl)-(1→6)-2-*O*-benzoyl-3,4-di-*O*-benzyl-α-D-mannopyranoside (**7**):

Following the general procedures for glycosylations, a glycosylation of mannosyl phosphate **5**[7] (339.4 mg, 0.417 mmol) and mannose **6**[7] (162.0 mg, 0.321 mmol) promoted by TMSOTf (82.1 µL, 0.417 mmol) was carried out in CH_2Cl_2 (0.6 mL) at 0 °C for 1.5 h. After being quenched by NEt_3 (100 µL), the reaction mixture was concentrated *in vacuo* and subjected to the silica gel column chromatography (Hexane/EtOAc = 3:2) to obtain compound **7** (227.0 mg, 75%) as a colorless syrup. The spectral data were in agreement with those in the literature.[40] HRMS-ESI (m/z): $[M+Na]^+$ calculated for $C_{57}H_{58}NaO_{13}$, 973.3775; Found: 973.3778.

Allyl *O*-(2-*O*-Benzoyl-3,4-di-*O*-benzyl-α-D-mannopyranosyl)-(1→6)-*O*-(2-*O*-benzoyl-3,4-di-*O*-benzyl-α-D-mannopyranosyl)-(1→6)-2-*O*-benzoyl-3,4-di-*O*-benzyl-α-D-annopyranoside (**3**):

Following the general procedures for glycosylations, a glycosylation of mannosyl phosphate **5** (209.2 mg, 0.257 mmol) and dimannoside **7** (203.9 mg, 0.214 mmol) promoted by TMSOTf (50.6 μL, 0.257 mmol) was carried out in CH_2Cl_2 (0.6 mL) at 0 °C for 45 min. After being quenched by NEt_3 (100 μL), the reaction mixture was concentrated *in vacuo* and subjected to flash silica gel column chromatography (Hexane/EtOAc = 3:2) to obtain compound **3** (197.0 mg, 66%) as a colorless syrup. R_f 0.30 (Hexane/EtOAc = 3:1); $[\alpha]_D^{r.t.}$ = +22.40 (*c* = 1.0, CH_2Cl_2); ^{1}H NMR (400 MHz, $CDCl_3$) δ 8.15-8.07 (m, 6H, Ar-*H*), 7.60-7.44 (m, 9H, Ar-*H*), 7.30-7.08 (m, 30 H, Ar-*H*), 5.94-5.84 (m, 1H, $CH_2CH{=}CH_2$), 5.82 (dd, *J* = 1.9, 3.1 Hz, 1H, *H2*), 5.75 (dd, *J* = 1.9, 3.1 Hz, 1H, *H2*), 5.69 (dd, *J* = 1.9, 3.1 Hz, 1H, *H2*), 5.29 (dd, *J* = 1.5, 17.2 Hz, 1H, $CH_2CH{=}CH_2$), 5.20 (dd, *J* = 1.4, 10.4 Hz, 1H, $CH_2CH{=}CH_2$), 5.10 (d, *J* = 1.5 Hz, 1H, *H1*), 5.04 (d, *J* = 1.5 Hz, 1H, *H1*), 4.98 (d, *J* = 1.6 Hz, 1H, *H1*), 4.92-4.39 (m, 12H), 4.20-3.60 (m, 17H); $^{13}C\{^1H\}$ NMR (100 MHz, $CDCl_3$) δ 165.6 (*C*OPh), 165.5 (*C*OPh), 165.3 (*C*OPh), 138.3, 138.3, 138.2, 137.8, 137.5, 133.2, 129.8, 128.5, 128.4, 128.2, 128.1, 127.9, 127.6, 127.4, 127.3, 118.0, 98.1 (*C1*), 97.9 (*C1*), 96.9 (*C1*), 78.5, 78.0, 77.6, 75.0, 74.0, 73.9, 73.6, 72.0, 71.5, 71.3, 71.1, 70.7, 68.9, 68.6, 68.4, 68.1, 66.0, 65.7, 61.7; HRMS-ESI (*m/z*): $[M+Na]^+$ calculated for $C_{84}H_{84}NaO_{19}$, 1419.5505; Found: 1419.5500.

Allyl *O*-(2-*O*-Acetyl-3,4,6-tri-*O*-benzyl-α-D-mannopyranosyl)-(1→6)-2-*O*-benzoyl-3,4-di-*O*-benzyl-α-D-mannopyranoside (**8**):

Following the general procedures for glycosylations, a glycosylation of mannosyl phosphate **1**[41,42] (300.5 mg, 0.439 mmol) and mannose **6** (147.6 mg, 0.293 mmol) promoted by TMSOTf (86 μL, 0.439 mmol) was carried out in CH_2Cl_2 (0.6 mL) at 0 °C for 20 min. After being quenched by NEt_3 (100 μL), the reaction mixture was concentrated *in vacuo* and purified by flash silica gel column chromatography (Hexane/EtOAc = 4:1) to obtain compound **8** (285.6 mg, 99%) as a colorless syrup. The spectral data were in agreement with those in the literature.[43] HRMS-ESI (m/z): $[M+Na]^+$ calculated for $C_{59}H_{62}NaO_{13}$, 1001.4088; Found: 1001.4080.

(2-*O*-Acetyl-3,4,6-tri-*O*-benzyl-α-D-mannopyranosyl)-(1→6)-2-*O*-benzoyl-3,4-di-*O*-benzyl-α-D-mannopyranose (**9**):

To a solution of compound **8** (266.4 mg, 0.272 mmol) in a mixture of acetic acid (6.0 mL) and water (0.3 mL), NaOAc (223.2 mg, 2.721 mmol) and $PdCl_2$ (241.3 mg, 1.361 mmol) were added. The reaction mixture was stirred at rt for 12 h. After the reaction had finished, the reaction was filtered through a pad of Celite and evaporated to dryness. The crude was extracted with EtOAc and saturated $NaHCO_3$ (3×100.0 mL). The solid Na_2CO_3 was added to carefully adjust the pH of the reaction mixture to 7. The combined organic layer was washed with saturated brine, dried over Na_2SO_4 and concentrated *in vacuo*. Purification of the crude by flash silica gel column chromatography (Hexane/EtOAc = 13:7) gave compound **9**[7] (221.6 mg, 87%) as a colorless syrup. R_f 0.33 (Hexane/EtOAc = 3:2); $[\alpha]_D^{r.t.}$ = + 0.18 (*c* = 1.0, CH_2Cl_2); ^{1}H NMR (300 MHz, $CDCl_3$) δ 8.09-8.07 (m, 2H, Ar-*H*), 7.52-7.42 (m, 3H, Ar-*H*), 7.29-7.10 (m, 25H, Ar-*H*), 5.63 (dd, *J* = 1.9, 3.0 Hz, 1H, *H2*), 5.45 (dd, *J* = 1.9, 3.0 Hz, 1H, *H2*), 5.25 (brs, 1H, *H1*), 4.96 (d, *J* = 1.4 Hz, 1H, *H1*), 4.89-4.41 (m, 10H), 4.17-3.60 (m, 11H), 2.13 (s, 3H, $COCH_3$); $^{13}C\{^1H\}$ NMR (75 MHz, $CDCl_3$) δ 170.6 ($COCH_3$), 165.8 (*C*OPh), 138.3, 138.0, 137.8, 133.3, 129.9, 128.5, 128.5, 128.4, 128.3, 128.2, 128.0, 127.8, 127.7, 98.2 (*C1*), 92.5 (*C1*), 78.2, 77.8, 75.2, 75.1, 74.4, 73.4, 71.6, 71.5, 70.8, 69.4, 69.1, 68.6, 67.7, 21.2 (CH_3); HRMS-ESI (*m/z*): $[M+Na]^+$ calculated for $C_{56}H_{58}NaO_{13}$, 961.3775; Found: 961.3769.

***N*-Phenyltrifluoroacetimidoyl *O*-(2-*O*-Acetyl-3,4,6-tri-*O*-benzyl-α-D-mannopyranosyl)-(1→6)-2-*O*-benzoyl-3,4-di-*O*-benzyl-α-D-mannopyranoside** (**4**):

N-phenyltrifluoroacetimidoyl chloride (103.7 µL, 7.645 mmol) was added to a solution of disaccharide **9** (151.3 mg, 0.161 mmol) in acetone (3.0 mL) at 0 °C, followed by cesium carbonate (105.0 mg, 0.322 mmol). The reaction was stirred overnight, allowing it to warm to rt. After the reaction had finished, it was filtered through a pad of Celite and evaporated to dryness. The crude was purified by flash silica gel column chromatography (Hexane/EtOAc = 4:1) to obtain compound **4** (152.3 mg, 85%) as a yellowish syrup. R_f 0.50 (Hexane/EtOAc = 7:3); $[\alpha]_D^{r.t.}$ = +37.16 (*c* = 1.0, CH_2Cl_2); ^{1}H NMR (300 MHz, $CDCl_3$) δ 8.11-8.09 (m, 2H, Ar-*H*), 7.51-7.45 (m, 3H, Ar-*H*), 7.34-7.04 (m, 28H, Ar-*H*), 6.84 (d, *J* = 7.8 Hz, 2H, Ar-*H*), 5.78 (brs, 1H, *H2*), 5.53 (brs, 1H, *H2*), 5.00 (brs, 2H, *H1*), 4.88-4.40 (m, 10H), 4.15-3.57 (m, 10H), 2.15 (s, 3H, $COCH_3$); $^{13}C\{^1H\}$ NMR (75 MHz, $CDCl_3$) δ 170.4 ($COCH_3$), 165.5 (*C*OPh), 143.2, 138.6, 138.3, 138.1, 137.8, 137.6, 133.6, 130.0, 129.6, 128.9, 128.8, 128.5, 128.4, 128.3, 128.2, 128.0, 127.9, 127.7, 127.6, 124.7, 119.6, 98.3, (*C1*), 94.6 (*C1*), 77.9, 75.5, 75.2, 74.2, 73.5, 72.2, 71.9, 71.6, 68.8, 68.4, 67.7, 66.0, 21.2 (*C*H_3); HRMS-ESI (*m/z*): $[M+Na]^+$ calculated for $C_{64}H_{62}F_3NNaO_{13}$, 1132.4071; Found: 1132.4025.

Allyl *O*-(2-*O*-Acetyl-3,4,6-tri-*O*-benzyl-α-D-mannopyranosyl)-(1→6)-*O*-(2-*O*-benzoyl-3,4-di-*O*-benzyl-α-D-mannopyranosyl)-(1→6)-*O*-(2-*O*-benzoyl-3,4-di-*O*-benzyl-α-D-mannopyranosyl)-(1→6)-*O*-(2-*O*-benzoyl-3,4-di-*O*-benzyl-α-D-mannopyranosyl)-(1→6)-2-*O*-benzoyl-3,4-di-*O*-benzyl-α-D-mannopyranoside (**10**):

Following the general procedures for glycosylations, a glycosylation of dimannosyl imidate **4** (370.0 mg, 0.333 mmol) and trimannoside **3** (310.5 mg, 0.222 mmol) promoted by TMSOTf (65.6 µL, 0.333 mmol) was carried out in CH_2Cl_2 (2.7 mL) at 0 °C for 30 min. After being quenched by NEt_3 (100 µL), the reaction mixture was concentrated *in vacuo* and purified by flash silica gel column chromatography (Hexane/EtOAc = 7:3) to obtain compound **10** (453.8 mg, 88%) as a colorless syrup. R_f 0.45 (Hexane/EtOAc = 7:3); $[\alpha]_D^{r.t.}$ = + 1.17 (*c* = 0.1, CH_2Cl_2); ^{1}H NMR (300 MHz, $CDCl_3$) δ 8.19-8.13 (m, 8H, Ar-*H*), 7.51-7.46 (m, 12H, Ar-*H*), 7.34-7.07 (m, 55 H, Ar-*H*), 5.95-5.87 (m, 1H, $CH_2CH{=}CH_2$), 5.84 (brs, 3H, *H2*), 5.70 (dd, *J* = 1.7, 2.8 Hz, 1H, *H2*), 5.58 (dd, *J* = 1.7, 2.8 Hz, 1H, *H2*), 5.29 (dd, *J* = 1.5, 17.2 Hz, 1H, $CH_2CH{=}CH_2$), 5.19 (dd, *J* = 1.1, 10.4 Hz, 1H, $CH_2CH{=}CH_2$), 5.14 (d, *J* = 1.0 Hz, 1H, *H1*), 5.09 (d, *J* = 0.9 Hz, 1H, *H1*), 5.06 (d, *J* = 1.0 Hz, 1H, *H1*), 5.00 (d, *J* = 1.2 Hz, 1H, *H1*), 4.99 (d, *J* = 1.4 Hz, 1H, *H1*), 4.95-4.34 (m, 22H), 4.20-3.49 (m, 27H), 2.14 (s, 3H, $COCH_3$); $^{13}C\{^1H\}$ NMR (75 MHz, $CDCl_3$) δ 170.4 (*C*OCH_3), 165.9 (*C*OPh), 165.7 (*C*OPh), 165.6 (*C*OPh), 165.6 (*C*OPh), 138.6, 138.3, 137.7, 133.4, 129.9, 128.7, 128.4, 128.3, 127.9, 127.7, 127.4, 118.2, 98.5 (*C1*), 98.3 (3×*C1*), 97.1, (*C1*), 78.7, 78.4, 77.9, 75.2, 74.3, 74.1, 74.1, 73.5, 71.8, 71.5, 71.1, 69.1, 68.7, 68.3, 66.2, 65.9, 65.8, 21.3 (*C*H_3); HRMS-ESI (*m/z*): $[M+Na]^+$ calculated for $C_{140}H_{140}NaO_{31}$, 2339.9276; Found: 2339.9285.

(2-*O*-Acetyl-3,4,6-tri-*O*-benzyl-α-D-mannopyranosyl)-(1→6)-*O*-(2-*O*-benzoyl-3,4-di-*O*-benzyl-α-D-mannopyranosyl)-(1→6)-*O*-(2-*O*-benzoyl-3,4-di-*O*-benzyl-α-D-mannopyranosyl)-(1→6)-*O*-(2-*O*-benzoyl-3,4-di-*O*-benzyl-α-D-mannopyranosyl)-(1→6)-2-*O*-benzoyl-3,4-di-*O*-benzyl-α-D-mannopyranose (**11**):

To a solution of compound **10** (261.7 mg, 0.113 mmol) in a mixture of acetic acid (7.5 mL), EtOAc (0.4 mL) and water (0.4 mL), NaOAc (92.6 mg, 1.129 mmol) and $PdCl_2$ (100.0 mg, 0.5650 mmol) were added. The reaction mixture was stirred at rt for 12 h. After the reaction had finished, the reaction was filtered through a pad of Celite and evaporated to dryness. The crude was extracted with EtOAc and saturated $NaHCO_3$ (3×100.0 mL). Solid Na_2CO_3 was added to carefully adjust the pH of the reaction mixture to 7. The combined organic layer was washed with saturated brine, dried over Na_2SO_4, and concentrated *in vacuo*. Purifying the crude by flash silica gel column chromatography (Hexane/EtOAc = 3:2) gave the desired compound **11** (217.0 mg, 85%) as a colorless syrup. R_f 0.50 (Hexane/EtOAc = 3:2); $[\alpha]_D^{r.t.}$ = +36.33 (*c* = 0.1, CH_2Cl_2); ^{1}H NMR (300 MHz, $CDCl_3$) δ 8.16-8.07 (m, 8H, Ar-*H*), 7.49-7.47 (m, 12H, Ar-*H*), 7.31-7.09 (m, 55H, Ar-*H*), 5.80 (brs, 3H, *H2*), 5.64 (brs, 1H, *H2*), 5.56 (brs, 1H, *H2*), 5.21-4.98 (m, 5H, *H1*), 4.92-4.31 (m, 22H), 4.17-3.46 (m, 25H), 2.15 (s, 3H, COCH_3); ^{13}C{^{1}H} NMR (75 MHz, $CDCl_3$) δ 170.4 (*C*OCH$_3$), 165.8 (*C*OPh), 165.8 (*C*OPh), 165.7 (*C*OPh), 165.6 (*C*OPh), 138.6, 138.4, 138.2, 137.7, 133.4, 129.9, 128.7, 128.5, 127.8, 127.7, 127.4, 98.5 (*C1*), 98.3 (*C1*), 98.2 (*C1*), 97.9 (*C1*), 92.7 (*C1*), 78.3, 78.2, 77.9, 75.2, 74.5, 74.1, 73.8, 73.5, 72.1, 71.7, 71.5, 71.0, 69.4, 68.6, 68.3, 66.4, 65.8, 26.5, 21.2 (*C*H$_3$); HRMS-ESI (*m/z*): $[M+Na]^+$ calculated for $C_{137}H_{136}NaO_{31}$, 2299.8963; Found: 2299.8955.

***N*-Phenyltrifluoroacetimidoyl *O*-(2-*O*-Acetyl-3,4,6-tri-*O*-benzyl-α-D-mannopyranosyl)-(1→6)-*O*-(2-*O*-benzoyl-3,4-di-*O*-benzyl-α-D-mannopyranosyl)-(1→6)-*O*-(2-*O*-benzoyl-3,4-di-*O*-benzyl-α-D-mannopyranosyl)-(1→6)-*O*-(2-*O*-benzoyl-3,4-di-*O*-benzyl-α-D-mannopyranosyl)-(1→6)-2-*O*-benzoyl-3,4-di-*O*-benzyl-α-D-mannopyranoside (12)**:

N-phenyltrifluoroacetimidoyl chloride (125.3 µL, 0.779 mmol) was added to a solution of pentasaccharide **11** (354.8 mg, 0.156 mmol) in acetone (7.7 mL) at 0 °C, followed by cesium carbonate (101.5 mg, 0.311 mmol). The reaction was stirred overnight, allowing it to warm to rt. After the reaction had finished, the reaction was filtered through a pad of Celite and evaporated to dryness. The crude was purified by flash silica gel column chromatography (Hexane/EtOAc = 7:3) to obtain compound **12** (248.4 mg, 65%) as a colorless syrup. R_f 0.45 (Hexane/EtOAc = 7:3); $[\alpha]_D^{r.t.}$ = +57.93 (*c* = 0.1, CH_2Cl_2); ^{1}H NMR (400 MHz, $CDCl_3$) δ 8.16-8.12 (m, 8H, Ar-*H*), 7.51-7.46 (m, 12H, Ar-*H*), 7.30-7.07 (m, 58H, Ar-*H*), 6.83 (d, *J* = 7.9 Hz, 2H, Ar-*H*), 5.81 (brs, 4H, *H2*), 5.56 (brs, 1H, *H2*), 5.09-4.91 (m, 5H, *H1*), 4.89-4.31 (m, 22H), 4.17-3.45 (m, 25H), 2.15 (s, 3H, COCH_3); ^{13}C{^{1}H} NMR (100 MHz, $CDCl_3$) δ 170.2 (*C*OCH$_3$), 165.6 (*C*OPh), 165.5 (*C*OPh), 138.5, 138.0, 137.6, 133.3, 129.8, 128.6, 128.3, 128.1, 127.7, 127.2, 119.4, 98.5 (*C1*), 98.4, (3×*C1*) 98.2 (*C1*), 78.2, 77.7, 75.0, 73.9, 73.3, 72.1, 71.6, 71.4, 70.9, 68.4, 67.5, 65.9, 65.6, 21.1 (CH_3); HRMS-ESI (*m/z*): $[M+Na]^+$ calculated for $C_{145}H_{140}F_3NNaO_{31}$, 2470.9259; Found: 2470.9229.

6-(*S*-Benzyl)thiohexyl *O*-(2-*O*-Acetyl-3,4,6-tri-*O*-benzyl-α-D-mannopyranosyl)-(1→6)-2-*O*-benzoyl-3,4-di-*O*-benzyl-α-D-mannopyranoside (**13**):

Following the general procedures for glycosylations, a glycosylation of dimannosyl imidate **4** (226.8 mg, 0.204 mmol) and 6-(benzylthio)-1-hexanol **2** (229.0 mg, 1.022 mmol), promoted by TMSOTf (60.0 μL, 0.307 mmol), was carried out in CH_2Cl_2 (0.7 mL) at -10 °C for 1 h. After being quenched by NEt_3 (60.0 μL), the reaction mixture was concentrated *in vacuo* and purified by size exclusion column chromatography (Sephadex LH-20, CH_2Cl_2/MeOH = 7:3) and by flash silica gel column chromatography (Hexane/EtOAc = 9:1) to obtain compound **13** (180.0 mg, 77%) as a yellowish syrup. R_f 0.55 (Hexane/EtOAc = 7:3); $[\alpha]_D^{r.t.}$ = +20.46 (*c* = 1.0, CH_2Cl_2); ^{1}H NMR (300 MHz, $CDCl_3$) *δ* 8.11-8.08 (m, 2H, Ar-*H*), 7.49-7.43 (m, 3H, Ar-*H*), 7.31-7.09 (m, 30H, Ar-*H*), 5.61 (dd, *J* = 1.8, 2.9 Hz, 1H, *H2*), 5.52 (dd, *J* = 1.8, 2.6 Hz, 1H, *H2*), 5.01 (d, *J* = 1.2 Hz, 1H, *H1*), 4.88 (brs, 1H, *H1*), 4.86-4.40 (m, 10H), 4.10-3.35 (m, 12H), 3.69 (brs, 2H), 2.40 (t, *J* = 7.5 Hz, 2H, CH_2SBn), 2.15 (s, 3H, $COCH_3$), 1.59-1.50 (m, 4H), 1.38-1.28 (m, 4H); $^{13}C\{^1H\}$ NMR (75 MHz, $CDCl_3$) *δ* 170.2 ($COCH_3$), 165.7 (*C*OPh), 138.5, 138.4, 138.3, 138.1, 137.9, 137.6, 133.2, 129.9, 129.8, 128.8, 128.5, 128.4, 128.3, 128.2, 128.1, 128.1, 128.0, 127.7, 127.6, 127.5, 127.4, 126.8, 97.9 (*C1*), 97.7 (*C1*), 78.5, 77.9, 75.1, 75.0, 74.1, 74.0, 73.3, 71.5, 71.4, 70.6, 69.0, 68.6, 68.3, 67.8, 66.1, 36.2, 31.2, 29.2, 29.0, 28.6, 25.7, 21.1 (CH_3); HRMS-ESI (*m/z*): $[M+Na]^+$ calculated for $C_{69}H_{76}NaO_{13}S$, 1167.4904; Found: 1167.4900.

6-(*S*-Benzyl)thiohexyl *O*-(3,4,6-Tri-*O*-benzyl-α-D-mannopyranosyl)-(1→6)-3,4-di-*O*-benzyl-α-D-mannopyranoside (**14**):

To a solution of compound **13** (65.4 mg, 0.057 mmol) in a mixture of CH_2Cl_2 and MeOH (2.0 mL each), NaOMe (12.4 mg, 0.228 mmol) was added. The reaction mixture was refluxed at 50 °C. After 12 h, the reaction was evaporated to dryness. The crude was purified by flash silica gel column chromatography (Hexane/EtOAc = 3:2) to obtain compound **14** (53.0 mg, 93%) as a colorless syrup. R_f 0.20 (Hexane/EtOAc = 3:2); $[\alpha]_D^{r.t.}$ = +46.37 (*c* = 1.0,

CH_2Cl_2); ^{1}H NMR (300 MHz, $CDCl_3$) δ 7.34-7.13 (m, 30H, Ar-*H*), 5.03 (brs, 1H, *H1*), 4.88-4.41 (m, 10H), 4.81 (brs, 1H, *H1*) 4.12-4.00 (brs, 2H, *H2*), 3.94-3.29 (m, 12H), 3.67 (brs, 2H), 2.38 (t, J = 7.3 Hz, 2H, CH_2SBn), 1.58-1.45 (m, 4H) 1.38-1.22 (m, 4H); ^{13}C{^{1}H} NMR (75 MHz, $CDCl_3$) δ 138.4, 138.2, 138.1, 137.9, 128.7, 128.4, 128.4, 128.3, 128.3, 128.2, 128.1, 127.8, 127.8, 127.7, 127.6, 127.4, 126.8, 99.7 (*C1*), 98.9 (*C1*), 80.3, 79.6, 75.0, 74.9, 74.1, 74.0, 73.3, 71.8, 71.6, 71.1, 70.5, 68.7, 68.2, 68.0, 67.5, 66.0, 36.2, 31.2, 29.1, 29.0, 28.5, 25.7; HRMS-ESI (*m/z*): [M+Na]$^+$ calculated for $C_{60}H_{70}NaO_{11}S$, 1021.4537; Found: 1021.4557.

6-(*S*-Benzyl)thiohexyl *O*-(2-*O*-{2-*O*-Acetyl-3,4,6-tri-*O*-benzyl-α-D-mannopyranosyl}-3,4,6-tri-*O*-benzyl-α-D-mannopyranosyl)-(1→6)-2-*O*-{2-*O*-acetyl-3,4,6-tri-*O*-benzyl-α-D-mannopyranosyl}-3,4-di-*O*-benzyl-α-D-mannopyranoside (**15**):

Following the general procedures for glycosylations, a glycosylation of dimannoside **14** (44.4 mg, 0.044 mmol) and mannosyl phosphate **1** (152.0 mg, 0.222 mmol) promoted by TESOTf (51.0 µL, 0.222 mmol) was carried out in Et_2O (3.0 mL) at 0 °C for 1 h. After being quenched by NEt_3 (60 µL), the reaction mixture was concentrated *in vacuo* and purified by flash silica gel column chromatography (Hexane/EtOAc = 7:3) and by size exclusion column chromatography (Sephadex LH-20, CH_2Cl_2/MeOH = 7:3) to obtain compound **15** (76.4 mg, 88%) as a colorless syrup. R_f 0.50 (Hexane/EtOAc = 7:3); $[\alpha]_D^{r.t.}$ = +229.57 (c = 1.0, CH_2Cl_2); ^{1}H NMR (400 MHz, $CDCl_3$) δ 7.33-7.10 (m, 60H, Ar-*H*), 5.54 (dd, J = 1.7, 3.1 Hz, 1H, *H2*), 5.53 (dd, J = 1.9, 3.0 Hz, 1H, *H2*), 5.08 (d, J = 1.9 Hz, 1H, *H1*), 5.07 (d, J = 1.8 Hz, 1H, *H1*), 4.92 (d, J = 1.5 Hz, 1H, *H1*), 4.76 (d, J = 1.2 Hz, 1H, *H1*), 4.86-4.32 (m, 22H), 4.05-3.17 (m, 24H), 3.66 (brs, 2H), 2.35 (t, J = 7.5 Hz, 2H, CH_2SBn), 2.10-2.09 (s, 6H, COCH_3), 1.53-1.40 (m, 4H) 1.32-1.16 (m, 4H); ^{13}C{^{1}H} NMR (100 MHz, $CDCl_3$) δ 170.1 (*C*OCH_3), 138.6, 138.6, 138.5, 138.2, 138.2, 138.2, 138.1, 138.0, 137.9, 128.8, 128.4, 128.4, 128.3, 128.3, 128.3, 128.2, 128.2, 127.9, 127.8, 127.8, 127.8, 127.7, 127.6, 127.5, 127.4, 127.4, 126.8, 99.6 (2×*C1*), 98.5 (*C1*), 98.4 (*C1*), 80.0, 79.8, 78.2, 78.1, 77.2, 75.2, 75.0, 75.0, 74.9, 74.8, 74.7, 74.6, 74.3, 74.2, 74.1, 73.4, 73.3, 73.1, 72.0, 71.9, 71.9, 71.8, 71.7, 71.6, 70.8, 68.9, 68.8, 68.7, 68.6, 67.4, 67.1, 36.2, 31.3, 29.2, 29.1, 28.7, 25.9, 21.1 (*C*H_3); HRMS-ESI (*m/z*): [M+Na]$^+$ calculated for $C_{118}H_{130}NaO_{23}S$, 1969.8621; Found: 1969.8616.

6-(*S*-Benzyl)thiohexyl *O*-(2-*O*-Acetyl-3,4,6-tri-*O*-benzyl-α-D-mannopyranosyl)-(1→6)-*O*-(2-*O*-benzoyl-3,4-di-*O*-benzyl-α-D-mannopyranosyl)-(1→6)-*O*-(2-*O*-benzoyl-3,4-di-*O*-

benzyl-α-D-mannopyranosyl)-(1→6)-*O*-(2-*O*-benzoyl-3,4-di-*O*-benzyl-α-D-mannopyranosyl)-(1→6)-2-*O*-benzoyl-3,4-di-*O*-benzyl-α-D-mannopyranoside (**16**):

Following the general procedures for glycosylations, a glycosylation of pentamannosyl imidate **12** (57.9 mg, 0.024 mmol) and 6-(benzylthio)-1-hexanol **2** (21.2 mg, 0.095 mmol) promoted by TMSOTf (8.4 µL, 0.043 mmol) was carried out in CH_2Cl_2 (0.5 mL) at -10 °C for 1 h. After being quenched by NEt_3 (10.0 µL), the reaction mixture was concentrated *in vacuo* and purified by size exclusion column chromatography (Sephadex LH-20, CH_2Cl_2/MeOH = 7:3) and by flash silica gel column chromatography (Hexane/EtOAc = 4:1) to obtain compound **16** (44.5 mg, 76%) as a colorless syrup. R_f 0.50 (Hexane/EtOAc = 7:3); $[\alpha]_D^{r.t.}$ = +39.20 (*c* = 1.0, CH_2Cl_2); ^{1}H NMR (400 MHz, $CDCl_3$) δ 8.19-8.14 (m, 8H, Ar-*H*), 7.51-7.46 (m, 12H, Ar-*H*), 7.34-7.10 (m, 60H, Ar-*H*), 5.84-5.67 (brs, 4H, *H2*), 5.58 (brs, 1H, *H2*), 5.14-4.99 (m, 5H, *H1*), 4.93-4.32 (m, 22H), 4.13-3.38 (m, 27H), 3.67 (brs, 2H), 2.39 (t, *J* = 7.6 Hz, 2H, CH_2SBn), 2.15 (s, 3H, $COCH_3$), 1.70-1.53 (m, 4H), 1.36-1.31 (m, 4H); $^{13}C\{^1H\}$ NMR (100 MHz, $CDCl_3$) δ 170.4 ($COCH_3$), 166.0 (*C*OPh), 165.7 (*C*OPh), 165.7 (*C*OPh), 165.6 (*C*OPh), 138.8, 138.6, 138.5, 138.3, 138.1, 137.8, 137.8, 137.7, 137.7, 133.4, 130.1, 130.0, 128.9, 128.8, 128.7, 128.6, 128.5, 128.5, 128.4, 128.4, 128.4, 128.3, 128.3, 128.2, 127.9, 127.9, 127.8, 127.7, 127.7, 127.4, 127.4, 127.3, 127.0, 98.5 (2×*C1*), 98.4 (*C1*), 98.3 (*C1*), 98.0 (*C1*), 78.8, 78.5, 78.4, 78.2, 77.9, 75.3, 75.2, 74.4, 74.2, 74.1, 74.0, 73.9, 73.5, 71.8, 71.6, 71.5, 71.4, 71.1, 71.0, 70.9, 69.2, 68.7, 68.6, 68.5, 68.4, 68.0, 66.2, 65.9, 65.8, 65.7, 36.4, 31.4, 29.4, 29.2, 28.8, 26.0, 21.3 (CH_3); HRMS-ESI (*m/z*): $[M+Na]^+$ calculated for $C_{150}H_{154}NaO_{31}S$, 2506.0092; Found: 2506.0058.

6-(*S*-Benzyl)thiohexyl *O*-(3,4,6-Tri-*O*-benzyl-α-D-mannopyranosyl)-(1→6)-*O*-(3,4-di-*O*-benzyl-α-D-mannopyranosyl)-(1→6)-*O*-(3,4-di-*O*-benzyl-α-D-mannopyranosyl)-(1→6)-*O*-(3,4-di-*O*-benzyl-α-D-mannopyranosyl)-(1→6)-3,4-di-*O*-benzyl-α-D-mannopyranoside (**17**):

To a solution of compound **16** (142.8 mg, 0.058 mmol) in a mixture of CH_2Cl_2 and MeOH (3.0 mL each), NaOMe (31.0 mg, 0.575 mmol) was added. The reaction mixture was refluxed at 50 °C. After 12 h, the reaction was evaporated to dryness. The crude was purified by size exclusion column chromatography (Sephadex LH-20, CH_2Cl_2/MeOH = 7:3) to obtain compound **17** (109.1 mg, 94%) as a colorless syrup. R_f 0.38 (CH_2Cl_2/MeOH = 19:1); $[\alpha]_D^{r.t.}$ =

Pd(+65.07 (c = 1.0, CH_2Cl_2); ^{1}H NMR (300 MHz, $CDCl_3$) δ 7.32-7.13 (m, 60H, Ar-*H*), 5.01-4.94 (m, 5H, *H1*), 4.88-4.41 (m, 22H), 4.11-3.99 (brs, 5H, *H2*), 3.88-3.28 (m, 27H), 3.66 (brs, 2H), 2.36 (t, J = 7.4 Hz, 2H, CH_2SBn), 1.88-1.41 (m, 4H), 1.36-1.18 (m, 4H); ^{13}C{^{1}H} NMR (75 MHz, $CDCl_3$) δ 138.5, 138.4, 138.3, 138.3, 138.2, 138.0, 137.9, 137.8, 137.8, 137.6, 128.7, 128.4, 128.4, 128.4, 128.3, 128.3, 128.2, 128.2, 128.1, 127.9, 127.8, 127.7, 127.6, 127.5, 127.4, 127.3, 126.8, 99.7 (*C1*), 99.0 (2×*C1*), 98.8 (*C1*), 98.7 (*C1*), 80.2, 79.8, 79.8, 79.5, 75.0, 74.9, 74.8, 74.7, 74.2, 74.1, 73.8, 73.3, 71.8, 71.6, 71.5, 71.4, 71.1, 70.7, 70.6, 70.1, 70.0, 68.8, 68.2, 67.4, 67.9, 65.9, 36.2, 31.2, 29.1, 29.0, 28.5, 25.8; HRMS-ESI (*m/z*): $[M+Na]^+$ calculated for $C_{120}H_{136}NaO_{26}S$, 2047.8938; Found: 2047.8972.

6-(*S*-Benzyl)thiohexyl *O*-(2-*O*-{2-*O*-Acetyl-3,4,6-tri-*O*-benzyl-α-D-mannopyranosyl}-3,4,6-tri-*O*-benzyl-α-D-mannopyranosyl)-(1→6)-*O*-(2-*O*-{2-*O*-acetyl-3,4,6-tri-*O*-benzyl-α-D-mannopyranosyl}-3,4,6-tri-*O*-benzyl-α-D-mannopyranosyl)-(1→6)-*O*-(2-*O*-{2-*O*-acetyl-3,4,6-tri-*O*-benzyl-α-D-mannopyranosyl}-3,4,6-tri-*O*-benzyl-α-D-mannopyranosyl)-(1→6)-*O*-(2-*O*-{2-*O*-acetyl-3,4,6-tri-*O*-benzyl-α-D-mannopyranosyl}-3,4,6-tri-*O*-benzyl-α-D-mannopyranosyl)-(1→6)-2-*O*-{2-*O*-acetyl-3,4,6-tri-*O*-benzyl-α-D-mannopyranosyl}-3,4-di-*O*-benzyl-α-D-mannopyranoside (**18**):

Following the general procedures for glycosylations, a glycosylation of pentamannoside **17** (101.2 mg, 0.050 mmol) and mannosyl phosphate **1** (342.0 mg, 0.499 mmol), promoted by TESOTf (28.7 μL, 0.125 mmol), was carried out in Et_2O (5.0 mL) at 0 °C for 25 min. After being quenched by NEt_3 (100 μL), the reaction mixture was concentrated *in vacuo* and purified by flash silica gel column chromatography (Hexane/EtOAc = 7:3) and by size exclusion column chromatography (Sephadex LH-20, CH_2Cl_2/MeOH = 7:3) to obtain compound **18** (132.2 mg, 60%) as a colorless syrup. R_f 0.73 (Hexane/EtOAc = 3:2); $[\alpha]_D^{r.t.}$ = +35.45 (c = 1.0, CH_2Cl_2); ^{1}H NMR (400 MHz, $CDCl_3$) δ 7.27-7.07 (m, 135H, Ar-*H*), 5.56-5.50 (brs, 5H, *H2*), 5.12-4.88 (m, 10H, *H1*), 4.84-4.23 (m, 52H), 4.14-3.05 (m, 57H), 3.64 (brs, 2H), 2.34 (t, J = 7.1 Hz, 2H, CH_2SBn), 2.09-1.99 (s, 15H, COCH_3), 1.66-1.43 (m, 4H), 1.28-1.21 (m, 4H); ^{13}C{^{1}H} NMR (100 MHz, $CDCl_3$) δ 170.0 (*C*OCH_3), 170.0 (*C*OCH_3), 169.9 (*C*OCH_3), 169.8 (*C*OCH_3), 169.7 (*C*OCH_3), 138.6, 138.6, 138.5, 138.4, 138.3, 138.2, 138.2, 138.1, 138.0, 137.8, 137.7, 128.7, 128.4, 128.2, 128.0, 127.9, 127.8, 127.8, 127.7, 127.6, 127.5, 127.4, 127.4, 127.3, 126.8, 99.9 (*C1*), 99.8 (*C1*), 99.7 (*C1*), 99.5 (*C1*), 99.3 (*C1*), 99.2 (*C1*), 99.0 (*C1*), 98.9 (*C1*), 98.8 (*C1*), 98.7 (*C1*), 80.0, 79.7, 79.6, 79.6, 79.2, 79.1, 78.5, 78.4, 78.3, 78.2, 75.0, 74.9, 74.8, 74.6, 74.2, 74.0, 73.3, 73.2, 73.1, 72.0, 71.8, 71.6, 69.0, 68.7, 68.6, 68.5, 67.4, 36.2, 31.2, 29.2, 29.0, 28.6, 25.8, 21.0, 20.9; HRMS-ESI (*m/z*): $[M+2Na]^{2+}$ calculated for $C_{265}H_{286}Na_2O_{56}S$, 2220.9524; Found: 2220.9544.

General Procedures for Birch Reductions

Each sample of the conjugated oligomannoside with a thiol linker (**13**, **15**, **16** and **18**, ~100 mg) was dissolved in dried THF (5.0 mL) in a three-neck round bottom flask. At -78 °C (dry ice/acetone bath), ammonia was condensed into the flask. Small pieces of sodium metal were added to generate a stable dark blue solution. The dark blue solution was stirred at -78 °C for 6 hours. The reaction was allowed to slowly warm up to rt. The remaining ammonia in the reaction solution was blown off by argon stream. The reaction solution was concentrated *in vacuo* and redissolved in DI water (10.0 mL). The solution was neutralized by adding a small amount of formic acid until it reached pH 7. The aqueous solution was extracted with CH_2Cl_2 (3×10.0 mL) to remove the less polar partially debenzylated side products and the remaining starting material. In case of **Man$_2$** and **BMan$_4$**, the remaining materials in the organic layer were subjected to Birch Reduction as described above. The aqueous layer containing the debenzylated products was dialyzed in DI water at 4 °C for 48 h to give the final products.

6-Thiohexyl *O*-(α-D-Mannopyranosyl)-(1→6)-α-D-mannopyranoside (**Man$_2$**):

Colorless solid (13.7 mg, 25%). $[\alpha]_D^{r.t.}$ = +15.47 (*c* = 0.1, Milli-Q water); mp = 179.1-183.2 °C; ^{1}H NMR (400 MHz, D_2O) δ 4.89-4.84 (brs, 2H, *H1*), 3.96-3.53 (m, 14H), 2.90 (t, *J* = 8.1 Hz, 0.58H), 2.76 (t, *J* = 7.0 Hz, 0.42H), 2.36 (t, *J* = 7.9 Hz, 1H), 1.77-1.54 (m, 4H), 1.47-1.37 (m, 4H); $^{13}C\{^1H\}$ NMR (100 MHz, D_2O) δ 99.9 (*C1*), 99.5 (*C1*), 72.7, 70.8, 70.6, 70.1, 68.0, 66.8, 65.8, 61.0, 60.8, 51.0, 28.3, 27.9, 27.4, 25.2, 23.9, 21.7; MS-MALDI (*m/z*): $[M+Na]^+$ calculated for $C_{18}H_{34}NaO_{11}S$, 481.1720; Found: 481.1739.

6-Thiohexyl *O*-(α-D-Mannopyranosyl)-(1→6)-*O*-(α-D-mannopyranosyl)-(1→6)-*O*-(α-D-mannopyranosyl)-(1→6)-*O*-(α-D-mannopyranosyl)-(1→6)-α-D-mannopyranoside (Man$_5$):

Colorless solid (12.3 mg, 27%). $[\alpha]_D^{r.t.}$ = +77.53 (*c* = 0.1, Milli-Q water); mp = 187.2-192.0 °C; ^{1}H NMR (400 MHz, D_2O) δ 4.87-4.83 (brs, 5H, *H1*), 3.97-3.52 (m, 32H), 2.89 (t, *J*

= 8.6 Hz, 0.58H), 2.75 (t, J = 7.0 Hz, 0.42H), 2.36 (t, J = 7.7 Hz, 1H), 1.76-1.53 (m, 4H), 1.46-1.35 (m, 4H); $^{13}C\{^1H\}$ NMR (100 MHz, D_2O) δ 99.9 (*C1*), 99.5 (*C1*), 99.3 (3×*C1*), 72.7, 70.9, 70.8, 70.7, 70.6, 70.5, 70.1, 70.0, 69.9, 68.0, 66.8, 66.7, 66.6, 65.7, 65.6, 65.5, 61.0, 60.7, 51.0, 38.2, 28.4, 28.3, 28.2, 27.9, 27.4, 27.1, 25.2, 25.0, 24.9, 23.9, 21.7; MS-MALDI (*m/z*): $[M+Na]^+$ calculated for $C_{36}H_{64}NaO_{26}S$, 967.3304; Found: 967.3343.

6-Thiohexyl *O*-(2-*O*-{α-D-Mannopyranosyl}-α-D-mannopyranosyl)-(1→6)-2-*O*-{α-D-mannopyranosyl}-α-D-mannopyranoside (**BMan₄**):

Colorless solid (11.7 mg, 33%). $[\alpha]_D^{r.t.}$ = +25.80 (c = 0.1, Milli-Q water); mp = 183.5-188.9 °C; ^1H NMR (400 MHz, D_2O) δ 5.12-5.01 (brs, 4H, *H1*), 4.06-3.52 (m, 26H), 2.91 (t, J = 8.0 Hz, 0.93H), 2.77 (t, J = 6.8 Hz, 0.53H), 2.36 (t, J = 7.8 Hz, 0.75H), 1.76-1.53 (m, 4H) 1.47-1.36 (m, 4H); $^{13}C\{^1H\}$ NMR (100 MHz, D_2O) δ 102.3 (2×*C1*), 98.3 (*C1*), 98.1 (*C1*), 78.7, 73.4, 73.2, 72.8, 71.2, 70.5, 70.4, 70.0, 69.9, 68.1, 66.9, 66.8, 66.7, 65.8, 61.1, 60.9, 51.0, 28.3, 28.2, 28.0, 27.4, 25.2, 25.0, 24.9, 23.9, 21.7; MS-MALDI (*m/z*): $[M+Na]^+$ calculated for $C_{30}H_{54}NaO_{21}S$, 805.2776; Found: 805.2798.

6-Thiohexyl *O*-(2-*O*-{α-D-Mannopyranosyl}-α-D-mannopyranosyl)-(1→6)-*O*-(2-*O*-{α-D-mannopyranosyl}-α-D-mannopyranosyl)-(1→6)-*O*-(2-*O*-{α-D-mannopyranosyl}-α-D-mannopyranosyl)-(1→6)-*O*-(2-*O*-{α-D-mannopyranosyl}-α-D-mannopyranosyl)-(1→6)-2-*O*-{α-D-mannopyranosyl}-α-D-mannopyranoside (**BMan₁₀**):

Colorless solid (15.4 mg, 31%). $[\alpha]_D^{r.t.}$ = +91.07 (c = 0.1, Milli-Q water); mp = 208.4-213.9 °C; ^1H NMR (400 MHz, D_2O) δ 5.11-4.90 (brs, 10H, *H1*), 4.07-3.56 (m, 62H), 2.91, (t, J = 8.0 Hz, 0.71H), 2.77 (t, J = 6.8 Hz, 0.72H), 2.39 (t, J = 7.2 Hz, 0.57H), 1.77-1.56 (m, 4H), 1.48-1.36 (m, 4H); $^{13}C\{^1H\}$ NMR (100 MHz, D_2O) δ 102.2 (5×*C1*), 98.3 (*C1*), 98.2 (4×*C1*), 78.8, 78.6, 73.3, 72.8, 71.2, 70.5, 70.3, 70.1, 68.1, 66.9, 66.7, 66.5, 65.8, 65.6, 61.1, 60.9, 51.0, 38.2, 28.3, 28.0, 27.5, 27.1, 25.2, 25.0, 23.9, 21.6; MS-MALDI (*m/z*): $[M+Na]^+$ calculated for $C_{66}H_{114}NaO_{51}S$, 1777.5945; Found: 1777.5980.

Mannan Microarrays to Determine Binding to DC-SIGN and MR

The synthetic glycans were immobilized on maleimide activated glass slides via their thiol handle following established protocols.[7,44] Amine-coated GAPS slides (purchased from

Corning) were incubated overnight at rt in a 35 mL DMF solution containing succinimidyl 4-(*N*-maleimidomethyl)cyclohexane-1-carboxylate (SMCC, 0.7 mM) and *N*,*N*-diisopropylethylamine (DIPEA, 100 mM). Then, the slides were washed four times with methyl alcohol and dried under a stream of argon. After preparing the maleimide functionalized surfaces, the synthetic glycans were immobilized on the slides using the following protocol: the synthetic glycans were treated with tris(2-carboxyethyl)phosphine (TCEP, 1 equiv.) in a PBS buffer (10 mM; pH, 7.4) for 1 h at rt. An array printer (NanoPrint 210 equipped with a 946MP10 stealth pin, Arrayit Corporation) was used to deliver as little as 3.9 nL/spot of the solutions containing carbohydrates that ranged in concentrations from 40 µM to 2,000 µM. Each concentration of a compound was spotted three times for technical replicates. Thereafter, the slides were stored in a humid chamber for 12 h at rt, then incubated for 1 h in a solution of 3-mercaptopropionic acid (1 mM) in 35 mL of the PBS buffer to quench all the remaining maleimide groups. The slides were washed three times with distilled water, and then twice with ethanol (95%). The slides were incubated for 1 h in a solution of 2.5% w/v BSA, then washed three times with PBST. The glass slides printed with the immobilized glycans were incubated with 30 µL solution of target protein (2 µg/100 µL, recombinant human DC-SIGN/CD209 Fc Chimera or recombinant human MR, purchased from R&D Systems) in a HEPES buffer (50 mM, pH 7.5) solution containing 1% BSA, 20 mM $CaCl_2$, and 0.5% Tween-20 at rt for 2 h to allow the protein to bind to the immobilized glycans. The excess protein was washed off thoroughly. The bound protein was incubated with 30 µL solution of fluorescein conjugated antibody (1 µg/100 µL, anti-human IgG Fc specific Cy3 purchased from Sigma-Aldrich or anti-human MR Alexa Fluor 647 purchased from Biolegend) in a HEPES buffer containing 1% BSA and 0.5% Tween-20 at rt for 1 h. The differences in protein binding affinity to synthetic glycans were assessed semi-quantitatively by monitoring fluorescence intensity via a fluorescence scanner (Genepix 4000B, Molecular Devices).

ACKNOWLEDGMENTS

This work was supported by the Thailand Research Fund (RSA6280106) and the National Vaccine Institute, Thailand. We thank Chulabhorn Research Institute for the required chemicals and equipment.

Supporting Information: Complete NMR spectral copies of all compounds and MALDI-TOF spectra.

REFERENCES

(1) "Global tuberculosis report 2018," Geneva: World Health Organization, 2018.

(2) Geijtenbeek, T. B.; Van Vliet, S. J.; Koppel, E. A.; Sanchez-Hernandez, M.; Vandenbroucke-Grauls, C. M.; Appelmelk, B.; Van Kooyk, Y. Mycobacteria target DC-SIGN to suppress dendritic cell function. *J. Exp. Med.* **2003**, *197*, 7-17.

(3) Kallenius, G.; Correia-Neves, M.; Buteme, H.; Hamasur, B.; Svenson, S. B. Lipoarabinomannan, and its related glycolipids, induce divergent and opposing immune responses to Mycobacterium tuberculosis depending on structural diversity and experimental variations. *Tuberculosis* **2016**, *96*, 120-130.

(4) Chatterjee, D.; Lowell, K.; Rivoire, B.; McNeil, M. R.; Brennan, P. Lipoarabinomannan of Mycobacterium tuberculosis. Capping with mannosyl residues in some strains. *J. Biol. Chem.* **1992**, *267*, 6234-6239.

(5) Mishra, A. K.; Driessen, N. N.; Appelmelk, B. J.; Besra, G. S. Lipoarabinomannan and related glycoconjugates: structure, biogenesis and role in Mycobacterium tuberculosis physiology and host–pathogen interaction. *FEMS Microbiol. Rev.* **2011**, *35*, 1126-1157.

(6) Guerin, M. E.; Korduláková, J.; Alzari, P. M.; Brennan, P. J.; Jackson, M. Molecular Basis of Phosphatidyl-myo-inositol Mannoside Biosynthesis and Regulation in Mycobacteria. *J. Biol. Chem.* **2010**, *285*, 33577-33583.

(7) Boonyarattanakalin, S.; Liu, X.; Michieletti, M.; Lepenies, B.; Seeberger, P. H. Chemical synthesis of all phosphatidylinositol mannoside (PIM) glycans from Mycobacterium tuberculosis. *J. Am. Chem. Soc.* **2008**, *130*, 16791-16799.

(8) Vignal, C.; Guérardel, Y.; Kremer, L.; Masson, M.; Legrand, D.; Mazurier, J.; Elass, E. Lipomannans, but not lipoarabinomannans, purified from Mycobacterium chelonae and Mycobacterium kansasii induce TNF-α and IL-8 secretion by a CD14-Toll-like receptor 2-dependent mechanism. *J. Immunol.* **2003**, *171*, 2014-2023.

(9) Birch, H. L.; Alderwick, L. J.; Appelmelk, B. J.; Maaskant, J.; Bhatt, A.; Singh, A.; Nigou, J.; Eggeling, L.; Geurtsen, J.; Besra, G. S. A truncated lipoglycan from mycobacteria with altered immunological properties. *Proc. Natl. Acad. Sci. U. S. A.* **2010**, *107*, 2634-2639.

(10) Dao, D. N.; Kremer, L.; Guérardel, Y.; Molano, A.; Jacobs, W. R.; Porcelli, S. A.; Briken, V. Mycobacterium tuberculosis Lipomannan Induces Apoptosis and Interleukin-12 Production in Macrophages. *Infect. Immun.* **2004**, *72*, 2067-2074.

(11) Stoop, E. J. M.; Mishra, A. K.; Driessen, N. N.; van Stempvoort, G.; Bouchier, P.; Verboom, T.; van Leeuwen, L. M.; Sparrius, M.; Raadsen, S. A.; van Zon, M.; van der Wel, N. N.; Besra, G. S.; Geurtsen, J.; Bitter, W.; Appelmelk, B. J.; van der Sar, A. M. Mannan core branching of lipo(arabino)mannan is required for mycobacterial virulence in the context of innate immunity. *Cell. Microbiol.* **2013**, *15*, 2093-2108.

(12) Mishra, A. K.; Alves, J. E.; Krumbach, K.; Nigou, J.; Castro, A. G.; Geurtsen, J.; Eggeling, L.; Saraiva, M.; Besra, G. S. Differential arabinan capping of lipoarabinomannan modulates innate immune responses and impacts T helper cell differentiation. *J. Biol. Chem.* **2012**, *287*, 44173-44183.

(13) Nigou, J.; Gilleron, M.; Cahuzac, B.; Bounéry, J.-D.; Herold, M.; Thurnher, M.; Puzo, G. The phosphatidyl-myo-inositol anchor of the lipoarabinomannans from Mycobacterium bovis bacillus Calmette Guerin Heterogeneity, structure, and role in the regulation of cytokine secretion. *J. Biol. Chem.* **1997**, *272*, 23094-23103.

(14) Osakwe, O. In *Social Aspects of Drug Discovery, Development and Commercialization*; *Academic Press*: Boston, 2016, p 109-128.

(15) Fraser-Reid, B.; Chaudhuri, S. R.; Jayaprakash, K. N.; Lu, J.; Ramamurty, C. V. S. Efficient Chemical Synthesis of a Dodecasaccharidyl Lipomannan Component of Mycobacterial Lipoarabinomannan. *J. Org. Chem.* **2008**, *73*, 9732-9743.

(16) Meester, W. J. N.; Van Maarseveen, J. H.; Kirchsteiger, K.; Hermkens, P. H. H.; Schoemaker, H. E.; Hiemstra, H.; Rutjes, F. P. J. T. Scope and limitations of the solution and solid phase synthesis of homoallylic amines via N-acyliminium ion reactions. *Arkivoc* **2004**, *2004*, 122-151.

(17) Yongyat, C.; Ruchirawat, S.; Boonyarattanakalin, S. Polymerization of mannosyl tricyclic orthoesters for the synthesis of α (1–6) mannopyranan—the backbone of lipomannan. *Bioorg. Med. Chem.* **2010**, *18*, 3726-3734.

(18) Leelayuwapan, H.; Kangwanrangsan, N.; Chawengkirttikul, R.; Ponpuak, M.; Charlermroj, R.; Boonyarattanakalin, K.; Ruchirawat, S.; Boonyarattanakalin, S. Synthesis and Immunological Studies of the Lipomannan Backbone Glycans Found on the Surface of Mycobacterium tuberculosis. *J. Org. Chem.* **2017**, *82*, 7190-7199.

(19) Hutacharoen, P.; Ruchirawat, S.; Boonyarattanakalin, S. Biological Activities of Synthetic Oligosaccharides and Glycolipids from Mycobacteria. *J. Carbohydr. Chem.* **2011**, *30*, 415-437.

(20) Ernst, J. D. The immunological life cycle of tuberculosis. *Nat. Rev. Immunol.* **2012**, *12*, 581-591.

(21) Dey, B.; Bishai, W. R. Crosstalk between Mycobacterium tuberculosis and the host cell. *Semin. Immunol.* **2014**, *26*, 486-496.

(22) Gibson, K. J.; Gilleron, M.; Constant, P.; Sichi, B.; Puzo, G.; Besra, G. S.; Nigou, J. A lipomannan variant with strong TLR-2-dependent pro-inflammatory activity in Saccharothrix aerocolonigenes. *J. Biol. Chem.* **2005**, *280*, 28347-28356.

(23) Quesniaux, V. J.; Nicolle, D. M.; Torres, D.; Kremer, L.; Guerardel, Y.; Nigou, J.; Puzo, G.; Erard, F.; Ryffel, B. Toll-like receptor 2 (TLR2)-dependent-positive and TLR2-independent-negative regulation of proinflammatory cytokines by mycobacterial lipomannans. *J. Immunol.* **2004**, *172*, 4425-4434.

(24) Puissegur, M. P.; Lay, G.; Gilleron, M.; Botella, L.; Nigou, J.; Marrakchi, H.; Mari, B.; Duteyrat, J. L.; Guerardel, Y.; Kremer, L.; Barbry, P.; Puzo, G.; Altare, F. Mycobacterial lipomannan induces granuloma macrophage fusion via a TLR2-dependent, ADAM9- and beta1 integrin-mediated pathway. *J. Immunol.* **2007**, *178*, 3161-3169.

(25) Nigou, J.; Vasselon, T.; Ray, A.; Constant, P.; Gilleron, M.; Besra, G. S.; Sutcliffe, I.; Tiraby, G.; Puzo, G. Mannan chain length controls lipoglycans signaling via and binding to TLR2. *J. Immunol.* **2008**, *180*, 6696-6702.

(26) Gagliardi, M. C.; Teloni, R.; Giannoni, F.; Pardini, M.; Sargentini, V.; Brunori, L.; Fattorini, L.; Nisini, R. Mycobacterium bovis Bacillus Calmette-Guerin infects DC-SIGN-dendritic cell and causes the inhibition of IL-12 and the enhancement of IL-10 production. *J. Leukoc. Biol.* **2005**, *78*, 106-113.

(27) Kerrigan, A. M.; Brown, G. D. C-type lectins and phagocytosis. *Immunobiology* **2009**, *214*, 562-575.

(28) Maeda, N.; Nigou, J.; Herrmann, J.-L.; Jackson, M.; Amara, A.; Lagrange, P. H.; Puzo, G.; Gicquel, B.; Neyrolles, O. The Cell Surface Receptor DC-SIGN Discriminates betweenMycobacterium Species through Selective Recognition of the Mannose Caps on Lipoarabinomannan. *J. Biol. Chem.* **2003**, *278*, 5513-5516.

(29) Schlesinger, L. S.; Hull, S. R.; Kaufman, T. M. Binding of the terminal mannosyl units of lipoarabinomannan from a virulent strain of Mycobacterium tuberculosis to human macrophages. *J. Immunol.* **1994**, *152*, 4070-4079.

(30) Schlesinger, L. S.; Kaufman, T. M.; Iyer, S.; Hull, S. R.; Marchiando, L. K. Differences in mannose receptor-mediated uptake of lipoarabinomannan from virulent and attenuated strains of Mycobacterium tuberculosis by human macrophages. *J. Immunol.* **1996**, *157*, 4568-4575.

(31) Martinez-Pomares, L. Exploiting Fc chimaeric proteins for the identification of ligands specific for the mannose receptor. *Methods Mol. Biol.* **2009**, *531*, 103-122.

(32) Taylor, M. E.; Bezouska, K.; Drickamer, K. Contribution to ligand binding by multiple carbohydrate-recognition domains in the macrophage mannose receptor. *J. Biol. Chem.* **1992**, *267*, 1719-1726.

(33) Adams, E. W.; Ratner, D. M.; Bokesch, H. R.; McMahon, J. B.; O'Keefe, B. R.; Seeberger, P. H. Oligosaccharide and glycoprotein microarrays as tools in HIV glycobiology; glycan-dependent gp120/protein interactions. *Chem. Biol.* **2004**, *11*, 875-881.

(34) Feinberg, H.; Castelli, R.; Drickamer, K.; Seeberger, P. H.; Weis, W. I. Multiple modes of binding enhance the affinity of DC-SIGN for high mannose N-linked glycans found on viral glycoproteins. *J. Biol. Chem.* **2007**, *282*, 4202-4209.

(35) Feinberg, H.; Mitchell, D. A.; Drickamer, K.; Weis, W. I. Structural basis for selective recognition of oligosaccharides by DC-SIGN and DC-SIGNR. *Science* **2001**, *294*, 2163-2166.

(36) Guo, Y.; Feinberg, H.; Conroy, E.; Mitchell, D. A.; Alvarez, R.; Blixt, O.; Taylor, M. E.; Weis, W. I.; Drickamer, K. Structural basis for distinct ligand-binding and targeting properties of the receptors DC-SIGN and DC-SIGNR. *Nat. Struct. Mol. Biol.* **2004**, *11*, 591-598.

(37) Blattes, E.; Vercellone, A.; Eutamene, H.; Turrin, C. O.; Theodorou, V.; Majoral, J. P.; Caminade, A. M.; Prandi, J.; Nigou, J.; Puzo, G. Mannodendrimers prevent acute lung inflammation by inhibiting neutrophil recruitment. *Proc. Natl. Acad. Sci. U. S. A.* **2013**, *110*, 8795-8800.

(38) Wattendorf, U.; Coullerez, G.; Voros, J.; Textor, M.; Merkle, H. P. Mannose-based molecular patterns on stealth microspheres for receptor-specific targeting of human antigen-presenting cells. *Langmuir* **2008**, *24*, 11790-11802.

(39) Yeeprae, W.; Kawakami, S.; Yamashita, F.; Hashida, M. Effect of mannose density on mannose receptor-mediated cellular uptake of mannosylated O/W emulsions by macrophages. *J. Control. Release* **2006**, *114*, 193-201.

(40) Heng, L.; Ning, J.; Kong, F. Facile synthesis of a comb-like mannohexaose: a trimer of the disaccharide repeating unit of the cell-wall mannans of Aphanoascus mephitatus and related species. *Carbohydr. Res.* **2001**, *331*, 431-437.

(41) Ravida, A.; Liu, X.; Kovacs, L.; Seeberger, P. H. Synthesis of glycosyl phosphates from 1,2-orthoesters and application to in situ glycosylation reactions. *Org. Lett.* **2006**, *8*, 1815-1818.

(42) Soldaini, G.; Cardona, F.; Goti, A. Catalytic Oxidation−Phosphorylation of Glycals: Rate Acceleration and Enhancement of Selectivity with Added Nitrogen Ligands in Common Organic Solvents. *Org. Lett.* **2005**, *7*, 725-728.

(43) Kwon, Y.-U.; Soucy, R. L.; Snyder, D. A.; Seeberger, P. H. Assembly of a Series of Malarial Glycosylphosphatidylinositol Anchor Oligosaccharides. *Chem.--Eur. J.* **2005**, *11*, 2493-2504.

(44) de Paz, J. L.; Horlacher, T.; Seeberger, P. H. Oligosaccharide microarrays to map interactions of carbohydrates in biological systems. *Meth. Enzymol.* **2006**, *415*, 269-292.

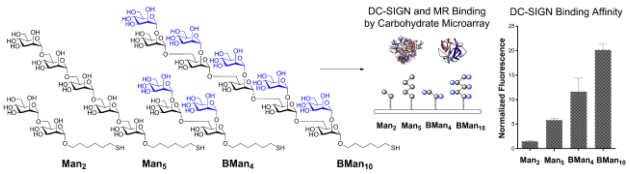
DC-SIGN and MR Binding
by Carbohydrate Microarray
DC-SIGN Binding Affinity
Normalized Fluorescence
0
5
10
15
20
25
Man2
Man5
BMan4
BMan10